DEVELOPMENT OF MODIFIED MTW ZEOLITES FOR CATALYTIC CRACKING OF N-HEXANE

BY

Mohammed Ahmed Sanhoob

A Thesis Presented to the

DEANSHIP OF GRADUATE STUDIES

KING FAHD UNIVERSITY OF PETROLEUM & MINERALS

DHAHRAN, SAUDI ARABIA

In Partial Fulfillment of the
Requirements for the Degree of

MASTER OF SCIENCE

In

CHEMICAL ENGINEERING

December, 2014

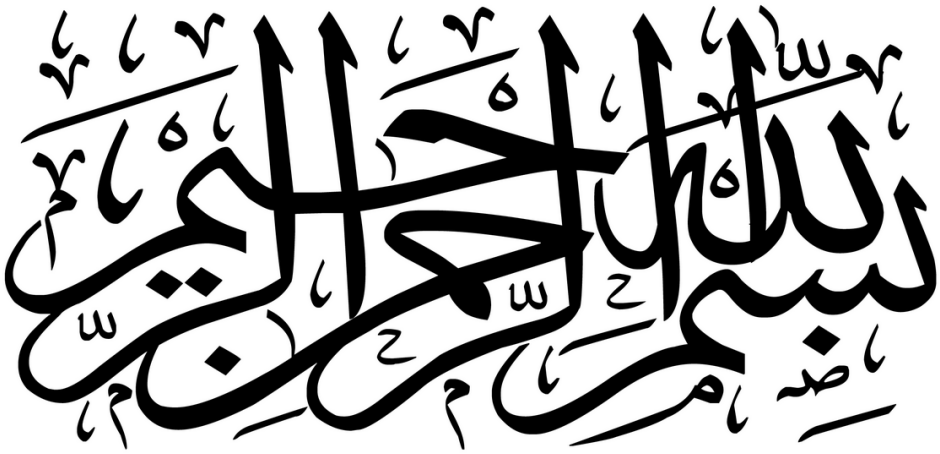

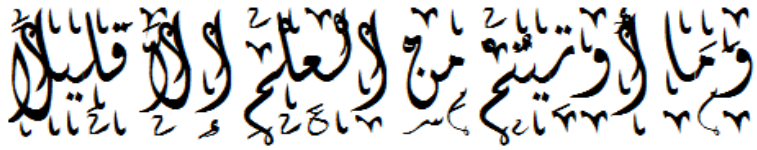

صدق الله العظيم

KING FAHD UNIVERSITY OF PETROLEUM & MINERALS

DHAHRAN- 31261, SAUDI ARABIA

DEANSHIP OF GRADUATE STUDIES

This thesis, written by **Mr. Mohammed Ahmed Sanhoob** under the direction his thesis advisor and approved by his thesis committee, has been presented and accepted by the Dean of Graduate Studies, in partial fulfillment of the requirements for the degree of **MASTERS OF SCIENCE IN CHEMICAL ENGINEERING.**

Oki Muraza

Dr. Oki Muraza
(Advisor)

Mozahar Hossain

Dr. Mohammad Mozahar Hossain
(Member)

Dr. Mohammed Ba-Shammakh
Department Chairman

Shaikh Abdur Razzak

Dr. Abdur Razzak Shaikh
(Member)

Dr. Salam A. Zummo
Dean of Graduate Studies

30/12/14

Date

Dedication

To my beloved parents who take my care, encouraged me and advised me.....

To my sisters and brothers who encouraged me throughout the duration of my studies.....

To all my family who stood beside me until I complete my degree.....

To all my teachers, lecturers and doctors who taught me during all my studies.....

To my wife and beloved son.....

To all of them, I dedicate this letter.

Mohammed Ahmed Sanhoob

ACKNOWLEDGMENTS

Firstly, I thank Allah and commend to him for his grace to me and bounty and very much reward and reconcile and facilitate to me all my duties until I got these results and completed all the required tasks.

After thanking Allah, I would like to thank King Fahd University of Petroleum and Minerals for giving me the chance for getting a Master degree from this great university. I would like also to thank the chemical engineering department and his Chairman, Graduate coordinator, faculty members and staff.

I would like also to thank Dr. Oki Muraza for his supervision, supporting me and for his continued advice and guide through my researches. I would like also to thank CENT and his director Dr. Zain Yamani for giving me the chance to do all my experiments in CENTs' labs. I would like also to thank all engineers, scientist and staff in CENT.

I would like also to thank the committee member for their support and advices. May ALLAH bless all of them and their families and give them a good and pleasant long life.

Mohammed Ahmed Sanhoob

TABLE OF CONTENTS

LIST OF TABLES

LIST OF FIGURES

LIST OF EQUATIONS

ABSTRACT

Full Name : Mohammed Ahmed Sanhoob

Thesis Title : Development of modified MTW zeolites for catalytic cracking of n-hexane

Major Field : Chemical Engineering

Date of Degree : December, 2014

The global demands for valuable oil products encouraged scientists to modify many catalysts needed in petrochemical industries such as zeolites. Zeolites with larger pore diameter such as ZSM-12 (MTW) is required to convert longer hydrocarbons. Numerous modifications have been applied to improve the properties of ZSM-12 zeolite. Most needed features in zeolite catalysts are the activity in catalytic cracking, the selectivity to olefin and the stability against the deactivation. For this purpose, ZSM-12 zeolite were modified to obtain pure phase of ZSM-12, and additional post-treatment to improve the stability of ZSM-12 in the steam environment. Pure ZSM-12 requires careful control of temperature, alkalinity and synthesis time. Elements such as lanthanum, cerium and boron were used to improve the hydrothermal stability of ZSM-12 zeolite. To evaluate the performance of modified ZSM-12, a model reaction of n-hexane cracking was applied. Boron doped ZSM-12 was superior as compared to conventional ZSM-12 as higher selectivities to propylene and ethylene were achieved with average selectivity to olefin of 71.7% with increase of 3.4% compare to the parent. Further test on the stability of the modified ZSM-12 zeolite samples were performed in hot liquid water and it was observed that the presence of boron enhanced the preservation of the crystallinity and desilication was happened in the framework of the zeolite.

ملخص الرسالة

الاسم الكامل: محمد أحمد يحي سنهوب

عنوان الرسالة: تطوير مادة إم تي دابليو المعدلة في تحويل وتكسير مادة الهكسان

التخصص: هندسة كميائية

تاريخ الدرجة العلمية: ديسمبر، 2014

الاحتياجات العالمية لمنتجات البترول القيمة شجعت العلماء الى تطوير الكثير من أنواع المحفزات و التي يتم استخدمها في الصناعات البتروكيماوية و خصوصا محفزات الزيوليت. الزيوليت ذات الحجوم الكبيرة مثل زد إس إم 12 (إم تي دابليو) يتم احتياجها لتحويل المواد الهيدروكربونية ذات السلسلة الطويلة. الكثير من التطويرات تم إضافتها إلى زد إس إم 12 لتطوير خواصها. أهم المميزات التي يجب توفرها في هذه المواد الزيوليتية هي حركية المادة المحفزة ومدى دقة اختيارها و كذلك مدى قدرتها على تحويل المواد المتفاعلة إلى منتجات مرغوبة مع الأخذ في الحسبان سرعة إبطال مادة الزيوليت. بسبب أهمية هذه المميزات، تم تطوير مادة زد إس إم 12 الزيوليتية لتحسين حركيتها وثباتها لمدة أطول خلال التفاعلات وتقليل مستوى إبطال المحفز. إن أنتاج مادة زد إس إم 12 النقي تتطلب الموازنة في درجة حرارة تحضيرها و مدى قلوية المادة ومدة التحضير. بعدما تمكنا من الحصول على زد إس إم 12 النقي، تم تلقيح المادة الناتجة بمواد فليزية مثل اللنثانوم و السيريوم النادرة و شبه الفلزية مثل البورون. بعد ذالك تم اختبار مدى فعالية المواد المطورة في تحويل و تكسير مادة الهكسان الى مواد كربونية مشبعة وغير مشبعة و خصوصا مادتي الإيثيلين و البروبيلين. من خلال النتائج، تبين أن اضافة مادة البورون الى المحفز الزيوليتي زد إس إم 12 زاد من مستوى مدى اختيارية المواد المرغوبة اثناء التفاعل وخصوصا إلى مادتي البروبيلين و الإيثيلين مع اختيارية عالية للمواد الكربونية غير المشبعة وصلت إلى 71.7% بزيادة 3.4% مقارنة بالمادة الغير المطورة. في اختبار اخر لمدى ثبات المواد في الماء الساخن، تبين كذلك أن المحفز الملقح بالبورون لديه ثبات أعلى و قابلية للأحتفاظ بالبلورات الأساسية لمدة أطول مع ملاحظة ازالة بعض جزيئات السيليكون من المحفز.

CHAPTER 1

INTRODUCTION

1.1. Olefin

Demands on valuable oil products over the world encouraged scientist to find new routes to produce chemicals with less economical costs. Chemicals such as olefin can be obtained from the catalytic cracking of naphtha. Naphtha in its current form, cannot be used unless it converted to lighter hydrocarbons. Valuable light hydrocarbons such as Olefin are highly preferable in refinery and petrochemical industries. Normally, catalytic cracking of naphtha can lead to olefin, paraffin and aromatics. However, selective catalysts are needed to enhance the selectivity towards the olefins rather than the other by-products. Olefins such as propylene and ethylene has highly demands due to the enlargement of the world. Propylene is a raw material for a wide range of chemicals such as propylene oxide, propylene glycol and polypropylene [1]. Ethylene is a raw material in the production of ethylene oxide, ethyl benzene and in the polymerization of polyethylene [2]. A model reaction of Naphtha is n-hexane. The physical as well as the chemical properties of n-hexane is shown in Table 1.1. In order to perform the catalytic cracking of Naphtha generally and n-hexane particularly, zeolitic materials are required.

Table 1.1: Physical properties of n-hexane [3].

Name	n-hexane
Molecular formula	C_6H_{14}
Molecular weight	86.17 g/mol
Vapor pressure (Pa)	20200
Solubility (g/m^3)	9.5

1.2. Zeolite catalysts

1.2.1. Background

Zeolite is a Greek word which means stone which boil. Zeolites can be found either in nature or it can be synthesized in laboratories and manufacturers. Zeolites are inorganic micro porous crystalline materials consists mainly of aluminum and silicates in tetrahedral (TO4) arrangement with O atoms connected to the adjacent tetrahedral [4, 5]. Where T is representing the Si and Al. Due to the repetition of these tetrahedra, silica is in the following form, SiO_2, which has a zero charge. Further addition of aluminum source which has +3, makes the overall charge of the zeolite framework to be negative [4]. Thus, additional cations are needed to neutralize the overall framework [4].

Mainly, zeolite synthesized by adding of aluminum source, silica source, cation source and sorbet phase [6]. Sorbet phases such as water and non-cationic organic are occupying the internal voids of the zeolite frameworks during the synthesis which can survive the intracrystalline pores (micro pores) after thermal treatment (calcination) [6]. Channels and cages host molecules such as water and organic solvents additional to cationic salts such as

alkali and alkaline-earth cations to stabilize zeolite frameworks and their structures as well as to facilitate the synthesis of the zeolites [6]. These salts will protonate through the thermal treatment which further can be exchanged with other elements such as hydrogen (H).

1.2.2. Zeolite impregnated with heteroatoms

Zeolite sometimes need to be modified with additional materials. This addition could modify the zeolite properties. These modifications can be applied by one of these methods: *in-situ* method or post-treatment method. If the modification is applied through the zeolite synthesis, then this is called *in-situ.* If the modification is applied after zeolites synthesis, then this is called post-treatment. Many researches have been carried out in many kinds of zeolites. Type of modification can be either by adding alcohol, polymeric materials, silane groups, semi metals or metals [7-13]. By such kind of modifications, changes such as Lewis or Brønsted sites, active sites, pore volume and surface area can be occurred. Catalytic properties such as conversion and selectivity in the reactions can be enhanced due to these modifications.

1.2.3. Role of mineralizer agent

Usually zeolites require a mineralizer agent during the synthesis. Most common mineralizer agent in zeolites is hydroxide group (OH^-). Sometimes, this mineralizer agent needs to be changed to get different properties in the synthesized zeolites. One of the most common mineralizer agents is the fluoride group (F^-). Modifying zeolite by partial or total replacement of a hydroxide group with the fluoride group can be either by *in situ* modification or post treatment (ion exchange) method. Adding the fluoride media as

mineralizer agent can add the hydrophobicity nature to the synthesized zeolite. Hydrophobic means unlike water.

1.2.4. ZSM-12 (MTW) zeolite

Demand to improve and modify different types of zeolite catalysts encouraged many scientists and many laboratories to improve the parameters of the synthesis of zeolites. Until now, there are more than 200 frameworks and more than 600 zeolites available and can be synthesized in laboratories [14]. It was targeted for many reactions such as hydrocarbon conversions, alkylation and isomerization [15]. The first synthesis of ZSM-12 zeolite was in 1974 by Mobil Research and Development scientists [16-18]. Its framework has a one-dimensional pore system and 12 membered-rings (MR) [19]. The pore size of MTW is 0.56 x 0.60 nm in the [010] plane, which is larger than MFI zeolites [14].

1.2.5. Desilication of zeolites

Zeolite can be modified with different methods. One of the modification methods is desilication. Desilication is a kind of post-treatment where some of silica atoms in the zeolite framework can be removed to form a hierarchical zeolite. Realization of the formation of hierarchical structures can be explained by the formation of mesoporosity in the zeolite crystal. To make a desilication process, basic solution is required [20]. The target from the desilication is to make easier internal transportation of the larger molecules to the active sites of the zeolites [21]. Desilication is proposed to improve the catalytic activity of the zeolite as well as the

catalytic effectiveness [22]. Zeolites such as ZSM-12 zeolite, which has one dimensional (1D) pore require a harsher alkaline treatment compared to 3D-pore zeolites [23]. Desilication can be performed under different kind of basic solution. It can be desilicated by sodium hydroxide solution or by other types of basic solution such as quaternary ammonium hydroxides. Quaternary solutions were proposed to produce the mesoporosity without losing the crystallinity of the hierarchical structure and the zeolite structures are stable [24]. Many zeolites were treated with different kinds of basic solutions such as ZSM-5, zeolite Y, ZSM-12, ZSM-22 and ZSM-23 and others [25-34].

1.2.6. Zeolite Stability

Many catalysts nowadays have been used in the petrochemical industry. Zeolites are among these catalysts which have been used. Reactions can happen in a wide temperature range. Some of these reactions, need high temperature, such as catalytic cracking. High temperature as an example, can affect zeolite stability. Many researches have been performed in order to obtain a stable zeolite in harsh condition. Before introducing the way of improving the stability of the zeolites, some classification of zeolites will be introduced. Zeolite can be classified based on the amount of aluminum into three parts [35]. These parts are low, medium and high silicon to aluminum ratios (Si/Al). Generally, zeolite assumed to be in low silicon to aluminum ratio when Si/Al is less than 5. Greater than that value and less than 10, it will be considered as a medium silicon to aluminum ratio. A further increase in the Si/Al ratio beyond 10, it will be considered as a high silica to aluminum ratio.

Depend on the type of the zeolite, the Si/ Al ratios can be varied between 1 and ∞. The hydrothermal stability and hydrophobicity increases as the silica to alumina ratio of the framework increases [36]. An optimum value is required for each kind of reaction to obtain a proper zeolite having both stability and hydrophobicity as well as higher conversion and selectivity. One of the proper techniques to increase the silica to aluminum ratio and so increasing the thermal stability of the zeolite is to replace inorganic bases with organic ones followed by the increase in these organic contents in a limited range as proposed by Barrer et al [37]. Another way to improve the thermal stability and the hydrophobicity nature of zeolite is to replace the hydroxide ions totally or partially with fluoride ions [38-40].

1.2.7. Zeolite acidity

One of the most important factors on the zeolites is their acidities. This acidity helps the transformation of the hydrocarbon [41]. Acidity can be donated either from Brønsted acid sites or Lewis acid sites. Normally, the strength of both weak and strong acidities can be evaluated using temperature-programmed desorption (TPD). To distinguish the quantity of Brønsted and Lewis acid sites, pyridine adsorption monitored by Fourier transform infrared spectroscopy (FTIR) is required.

1.2.8. Zeolite deactivation

Deactivation phenomenon can be happened from several factors. One of these factors is the coke deposition on the active sites and pore plugging during the reaction. Cokes as well as

the inaccessibility or blockage of the active sites are the most reason to the deactivation of the zeolite [6, 37]. Another factor that affects the deactivation rate is the structural collapse.

1.2.9. Application of ZSM-12 zeolite

ZSM-12 zeolite has been used in different fields in petrochemical industries. It was used for long hydrocarbon conversion due to its activity with time and perfect stability [42-44]. ZSM-12 zeolite was used in the isomerization of aromatic, alkylation of 2,6-dimethylnaphthalene and cracking of different kind of hydrocarbons [45-47]. Various transformations of hydrocarbon in petroleum refining, such as hydrocracking, alkylation, isomerization and cracking are due to the acid form of ZSM-12 [48]. In thesis, ZSM-12 zeolite was applied in the cracking of n-hexane. N-hexane is the model compound of naphtha. Generally, Naphtha consists of C5-C8 hydrocarbons.

CHAPTER 2

LITERATURE REVIEW

2.1. Applications of zeolites

Nowadays, zeolites are the most important material used in many fields overall the world. This wide application of zeolites is due to its importance to the global market. Zeolites are used in petrochemical refining industries, water purification, nuclear industry, biogas industries, detergents, toothpaste, agriculture and construction [15, 49-55]. In petrochemical industries, zeolites were used in many processes such as alkylation, isomerization, catalytic cracking of hydrocarbon and hydrocracking [56-59].

A process where one alkali group transfers to another alkali group is called alkylation. As an example of this reaction is the alkylation of benzene with propylene to produce cumene. The process where a certain molecule is rearranged in different arrangement is called isomerization. Another important topic is to crack long hydrocarbon molecules into smaller molecules. The importance of improving this field is coming from the huge production from oil reservoirs which increase with time. Due to huge consuming, lighter hydrocarbons quantities are decreasing with time and the heavier hydrocarbons are increasing. The lighter hydrocarbons can be used in many fields in industries. However, the heavier hydrocarbons can’t be used unless they are transformed or cracked to lighter hydrocarbons. As a result,

modifying the reaction route or catalytic properties are required to get higher selectivity as well as higher conversion.

2.2. Cracking mechanism

The reaction mechanism for n-hexane cracking is well established as shown in Figure 2.1. The reaction will start by the formation of carbonium ion on the Brønsted acid sites through the protonation step [60]. Then subsequence steps of protonation will follow the formation of the carbonium ion. The unstable carbonium ion will decompose to low alkane or hydrogen and carbenium ion which will adsorbed on the zeolite surface. Then the reaction will propagate. This reaction of carbenium ion will include dehydration, isomerization, β-scission and hydride transfer [60]. High temperature and less aluminum content are claimed to be a demand for the protolytic route in n-hexane cracking [61].

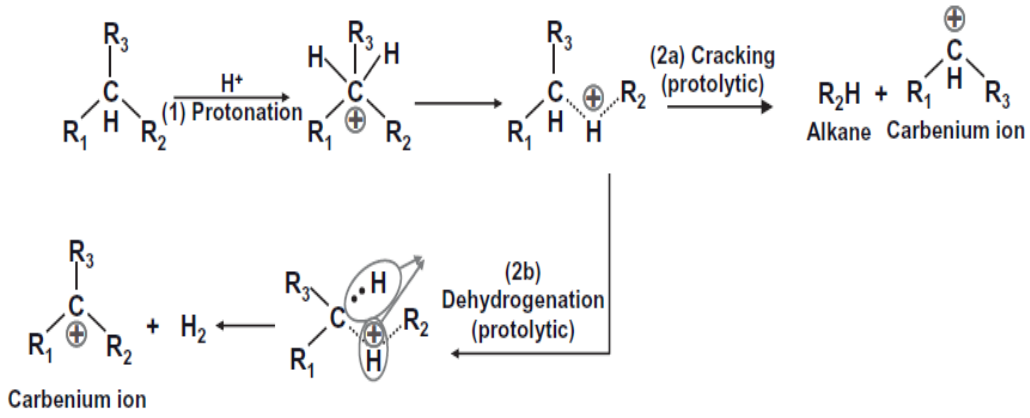

Figure 2.1:Monomolecular protolytic mechanism [60].

As an example, the mechanism of n-hexane cracking can be expanded as shown in Figure 2.2.

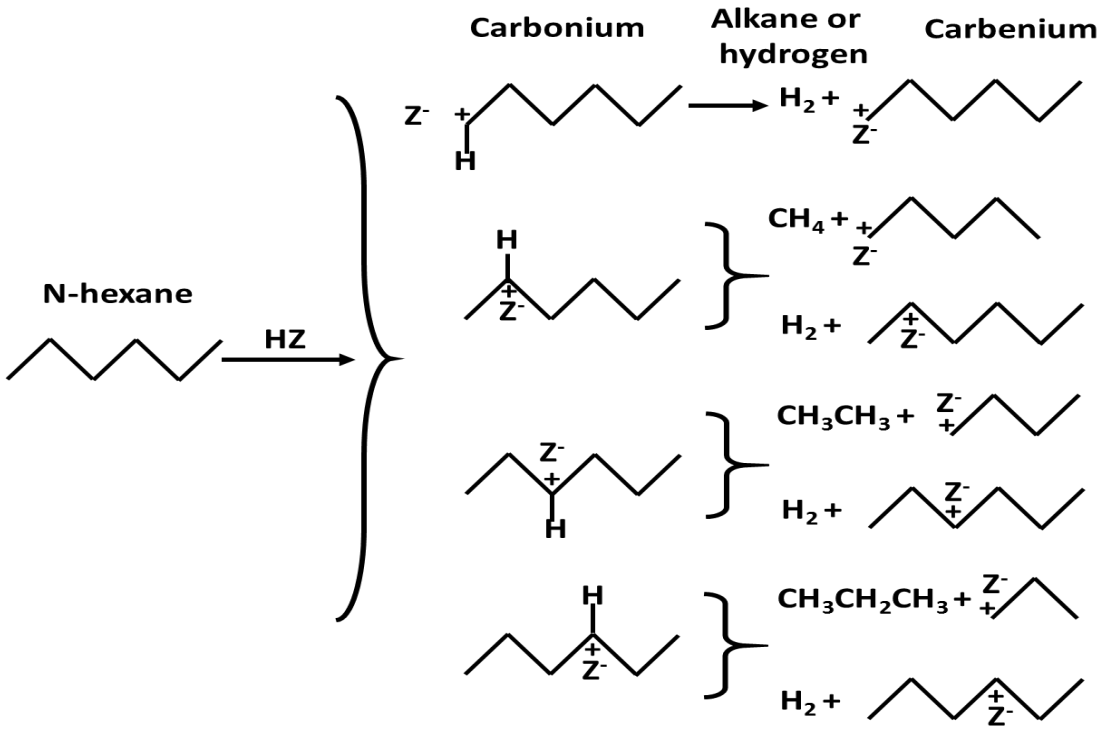

Figure 2.2: Reaction mechanism of n-hexane.

2.3. Framework structure of zeolites

Materials can be either amorphous or crystalline. In crystalline materials, atoms will arrange and repeat themselves over large atomic distances. The atoms will locate themselves in a repetitive three dimensional arrangement in which each atom is bonded to its nearest neighbor atoms. However, the amorphous material is not arranged in repetitive form.

Zeolites are crystalline materials. In zeolites, the main factor which makes one zeolite differ from another zeolite is the type of crystal structure. Zeolite frameworks are characterized with atoms connected with each other where the silicon atoms are located in the middle and the atoms of oxygen are located at the corners. The connection of each framework with the other frameworks is from their corners to form a tetrahedron. The form of the tetrahedra in zeolites is TO4 where T is either Si ‘silica’ or Al ‘aluminum’. Sometimes other atoms such as iron, gallium, cobalt and others can be added and represented as T atom. Generally, the structure of the zeolite can be displayed as shown in Figure 2.3:

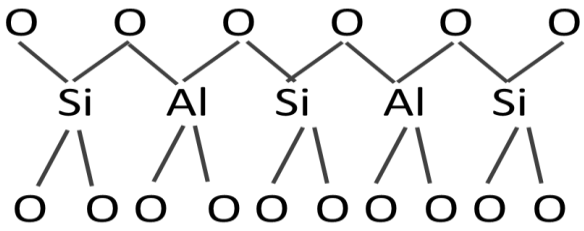

Figure 2.3: Distribution of the molecules and their connections.

The framework of the zeolite is negatively charged due to the presence of the Al atoms which has +3 charges. As a result, the framework requires an extra cationic framework such as sodium, potassium, barium, calcium, water, ammonia and carbonate ions to keep the overall framework neutral. The frameworks of the zeolites have linked cages, cavities or channels. As an example, in ZSM-12 zeolite, these channels and cages have limited pore sizes which are roughly between 0.3 and 0.8 nm in diameter [62]. Some examples for zeolites cages and channels are shown in Figure 2.4.

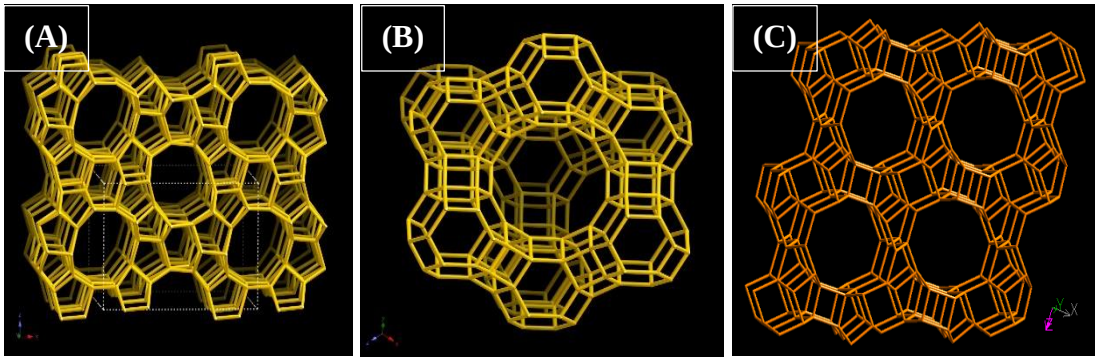

Figure 2.4: Different type of zeolite framework [63]. (A) MFI, (B) FAU, (C) MTW.

The empirical formula of all zeolites can be described as follows:

$$M^{n+}{}_{1/n}.\ A102^{-}.\ x\ Si0_2.\ y\ H_2O$$

Where: M: counter ion, n: counter ion valence, x: silicon/aluminum ratio, y: content of hydrate water [6, 64, 65].

The crystal type of ZSM-12 zeolite is monoclinic and the building unit cell has the following lattice parameters: a≠b≠c and the angle of each face is α= ɣ =90^o ≠ β. These dimensions are as follows: a=2.488 nm, b=0.502 nm, c=1.215 nm and the angles are α= ɣ =90 ^{o} and β=107.7^o [66]. The building unit of ZSM-12 zeolite is shown in Figure 2.5.

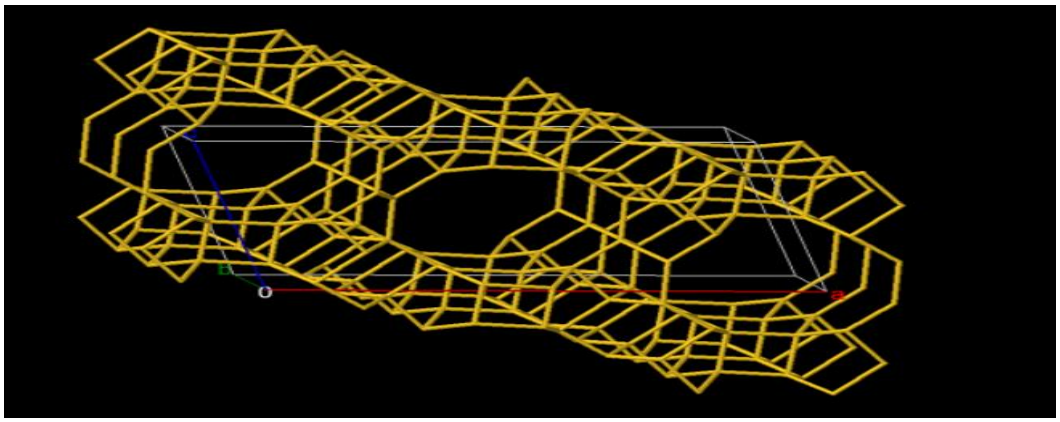
Figure 2.5: Building unit cell of ZSM-12 zeolite [67].

2.4. Hydrothermal synthesis of zeolite

The synthesis of zeolites can be performed using different methods. One of these methods is microwave assisted hydrothermal synthesis. In this method, shorter synthesis time can be expected. However, this method is not preferable for the zeolites which need more than 24 h of synthesis time because of the short time range operation demand for this machine. The most common and famous method of zeolite synthesis for different zeolites is the conventional hydrothermal synthesis. In this method, the synthesis gel or solution has to be replaced in PTFE reactor line stainless steel autoclave. The autoclave can be either static or in dynamic mode. Static means the synthesis is run without aging or stirring. However, in the dynamic mode, the synthesis is run under vibration, aging, rotating or stirring condition. Zeolite can be synthesized by static or dynamic hydrothermal oven or under microwave irradiation. Synthesis with hydrothermal oven usually takes longer time comparing with the one synthesized under microwave irradiation. A comparison between these two methods of heating is shown in Table 2.1.

Table 2.1: Differences between hydrothermal oven and microwave.

	Hydrothermal	**Microwave**
Synthesis time [68]	Longer	Shorter
Particle shape [68]	Less uniform	More uniform
Particle size [68, 69]	Longer	Shorter
Nucleation [69-72]	Slow	Fast
Product compositions [68, 73]	Less variable	More variable
Metal incorporation [74, 75]	Narrower range	Wider range

2.5. Effect of synthesis parameters on the zeolite properties

2.5.1. Effect of Si/Al ratio

Zeolite can be affected with different parameters. One of the most common factors which may affect the synthesis of the zeolite is the silicon to aluminum ratio (Si/Al). The importance of silicon to aluminum ratio can be shown from the importance of zeolite acidity.

As it is known, zeolites have two types of acidity. One of these acidities is called Lewis acid and the other is Brønsted acid. From this point, we can clarify the relation between the aluminum content and the acidity. Aluminum is Lewis acid. As a result, adding more aluminum means more Lewis acid and the vice versa. And from hydrocarbon cracking, it was noticed that the more aluminum content lead to the random cracking which led to less selectivity to the desired product [76]. So, an optimum amount of aluminum is required for each kind of reaction.

In zeolite synthesis, tuning the aluminum contents can affect the phase purity of the zeolites. The silica to aluminum ratio was studied in different types of zeolites such as NaX, MTW, MFI and mordenite [77-80]. In zeolite NaX, it was noticed that at very low Si/Al ratio amorphous was obtained. However, further increase in the Si/Al ratio led to the pure phase of NaX zeolite. Then after a further increase in the Si/Al ratio, impurities were appeared [77]. Xu Zhang et al showed the results as shown in Figure 2.6.

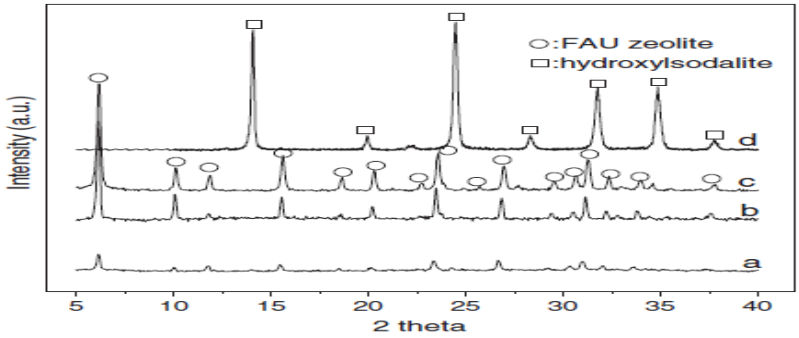

Figure 2.6: XRD results of zeolite NaX at different Si/Al [77].

In mordenite zeolite, it was noticed that as the silica to aluminum ratio increases, the analcime appears as an impurity phase at very low Si/Al ratio. They also noticed that the crystal size was decreased when they reduced the Si/Al ratio [80].

2.5.2. Effect of alkalinity

One of the main contents in zeolites synthesis is the alkaline source. The alkaline source is coming from alkali group which is connected with mineralizer agent. Most common alkali elements used are lithium (Li), sodium (Na) and potassium (K) in which one of these alkali metals is connected with the mineralizer agent [15, 81]. It was noticed that the potassium hydroxide needs longer crystallization time than sodium hydroxide in the synthesis of MTW zeolite [15].

Alkaline source plays an important role in crystallization rate as well as the phase purities of many kinds of zeolites. Tuning the alkalinity concentration can lead to producing zeolites with pure phase. The effect of alkalinity was studied with different types of zeolites such as

ZSM-12, mordenite and zeolite beta [15, 82]. In ZSM-12 zeolite, Yoo et al reported that at very low alkalinity, amorphous materials can be obtained. Increasing the alkalinity contents led to the pure ZSM-12 zeolite. A further increase in the alkalinity concentration led to the phase impurities such as cristobalite and amorphous as shown in Figure 2.7 [15].

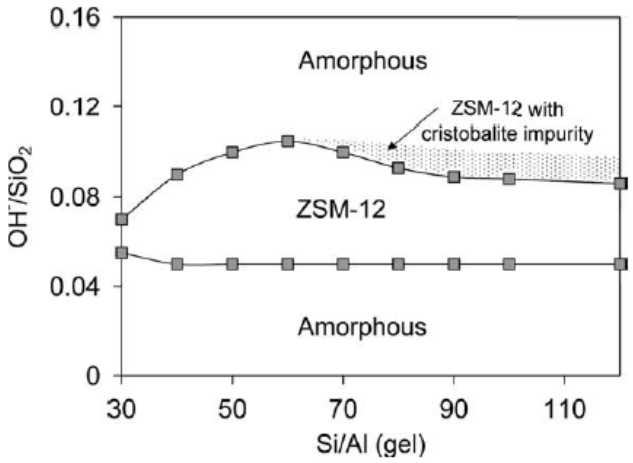

Figure 2.7: Domain of pure ZSM-12 zeolite using TEABr and $NaAlO_2$ as template and aluminum source respectively [15].

Effect of alkaline source was also reported for zeolite beta. Zaiku et al noticed that the alkalinity concentration can affect significantly the crystallinity and particle size. The alkalinity was noticed to be related to the Si/Al in the framework [82]. In mordenite zeolite, Mohamed et al noticed that the increase of alkalinity led to the higher in zeolite crystallinity [83].

2.5.3. Role of fluoride media to zeolite modifications

Zeolites usually synthesized under basic conditions. This basicity allows silica and alumina or other T atoms to dissolve and be ready for reaction by providing T-O-T hydrolysis [37].

Most common mineralizer agent is OH^- ion. However, some other mineralizer agents were also used in zeolite synthesis such as F^- [84, 85]. This fluoride ion can provide an advantage in zeolite synthesis by enable the acidic or nearly neutral crystallization of zeolite [86]. Nowadays, many salts were obtained in fluoride media such as MFI, TON, FER and MTT [37]. Many chemicals can be used as fluoride source such as ammonium fluoride (NH_4F), potassium fluoride (KF), sodium fluoride (NaF) and hydrofluoric acid (HF).

The importance of zeolite in the presence of fluoride source can be described by increasing the stability of the zeolite to be used in reactions such as steam cracking. Fluoride ion can add the feature of hydrophobicity to the zeolites as shown with numerous zeolites such as hydrophobic siliceous ferrierites and zeolite Beta [38, 87]. Thermal stability of zeolite can be studied using hot water. Until now, there is no any study for MTW zeolite stability when the fluoride media are used as mineralizer agent. Kalvachev et al compared the total loss for both fluoride and hydroxide media using TG [38]. Kalvachev et al noticed that fluoride media have less loss in weight as shown in Table 2.2.

Table 2.2: Zeolite made in fluoride media has less loss in TG than the one made in hydroxide media as shown by Kalvachev et al [38].

weight loss determined by TG						
Sample	Heating in Ar				Heating in Air	Total Loss, %
	303-493 K		493-873 K		At 873 K	Over 493 K
	T_{max}	% Loss	T_{max}	% Loss	% Loss	in Ar + Air
Beta-OH	363 K	8.9	733 K	3.2	2.85	6.05
Beta-F	360 K	8.4	813 K	3.7	0.16	3.86

2.5.4. Zeolite impregnated with metals

Zeolites can be exchanged with ammonium nitrate ($NH_4(NO_3)$) to get H-Zeolite after calcining the exchanged zeolite. Sometimes, this H-zeolite need to be impregnated with other elements such as lanthanum (La), cerium (Ce) and yttrium (Y) for a certain purpose depend on the features that need to be gained. As mentioned earlier, our purpose is to get a hydrophobic zeolite with higher thermal stability. In our experiments, we will add lanthanum and cerium. The addition of these metals was with different methods such as ion exchange or impregnation. One of these methods is by ion exchanging the elements. Lanthanum has two different oxidation state, +3 and +2. Different zeolites were impregnated with lanthanum and evaluated with different kind of reaction. An example of some zeolites impregnated with lanthanum is beta zeolite, zeolite Y and ZSM-5 [13, 88, 89].

In beta zeolite which was studied by Dalla et al [13], it was found that the zeolite was activated for the dehydration of glycerol. It was also noticed that the internal surface of the zeolite was blocked quickly and the rest of the reaction was based on the outer surface of the zeolite. This blockage was caused by the formation of coke. The XRD patterns of the exchanged zeolites were noticed to be with less crystallinity than that of the parent zeolite.

In ZSM-5 zeolite which was studied by Jiang et al [89], it was noticed that the acidities were slightly decreased by lanthanum treatment. It was also noticed that ZSM-5 treated with lanthanum activate the formation of the carbenium in the 1-butene reaction.

Cerium has three different oxidation state, +4, +3 and +2. Different zeolites were impregnated with cerium and evaluated with different kind of reaction. An example of some zeolites impregnated with cerium is zeolite Y and ZSM-5 zeolite [90-92].

In zeolite Y which was studied by Jezreel et al [92], they were noticed that the surface area was high. It was also noticed that it has higher catalytic activity and CO_2 yield in the oxidation of ethanol. Edward et al [90] noticed that the hydroxycerium molecules are formed at low temperature calcination up to 250°C. However, they believed that the compounds will convert to oxycerium complexes under the oxidation and dehydration conditions when the calcination temperature pass 300°C.

2.5.5. Zeolite impregnated with boric acid

Zeolite as mentioned earlier, composed of aluminum source beside the silica and alkaline sources. Sometime this aluminum source needs to be reduced and substituted with other elements in the zeolite crystal. This replacement can promote the feature of zeolite crystal. Tuning the acid site is a demand for some reactions. As known, that Brønsted acid sites can be varied based on the aluminum content variation. By reducing these aluminum atoms or exchanging them with other element such as boron, enhancement of the reduction of Lewis acid and so increases in Brønsted acid. Many compounds can be used as boron source. To get boron element, boric acid (H_3BO_3) will be used for producing H-B-zeolite. In literature, many works have been done in which boron atom was utilized in zeolite synthesis. An example of these zeolites, BEA zeolites, ZSM-5 and ZSM-11 [93-95]. It was reported that

the free boron zeolite was stable until 900 ^{o}C for ZSM-5 while the boron zeolite stability reached to 700 ^{o}C. However, further increase in temperature beyond 700 ^{o}C led to conversion in phase to cristobalite from ZSM-5 [94]. Generally, such kind of material will be added to study its effect on the thermal stability of the zeolites.

2.6. Cracking of n-hexane over zeolites

Most materials were used for cracking is the heavy oil, which has a long chain of hydrocarbon. An example of cracking is the cracking of n-hexane into shorter chains to get lighter hydrocarbons. This light hydrocarbon can be used in many fields such as polymerization of ethylene and propylene. The selectivity and conversion still the remaining topic that needs more investigation. Improving the catalyst can improve the selectivity, conversion and the stability of the catalyst in the hot stream. Different zeolites can be used for n-hexane cracking such as ZSM-5, ZSM-22, ZSM-23 and zeolite Y [28, 96].

Several parameters can affect the catalytic cracking of *n*-hexane over zeolites. These parameters can be classified to different classifications. Parameters based on the zeolite properties such as silica to aluminum ratio (Si/Al), crystal size, type of crystal, pore size, surface area and the acidity of the zeolite. Other parameters based on the reaction conditions such as steam, pressure, temperature, weight of the catalysts, flow rate of the feed and the

inert flow rate. These parameters can enhance the selectivity to certain products and the conversion.

For instance, Konno et al [97] evaluated the n-hexane cracking over ZSM-5 zeolite at different Si/Al ratio, different crystal size and different temperature. They found that small crystal size (nano) was more stable than the large crystal size (macro) due to the mass transfer limitation.

Zeolite modification can add a visible improvement in the selectivity or conversion of the reactants. Modification such as impregnation or ion exchange with metal or semi-metal was performed over different type of zeolites such as ZSM-5, zeolite Y and SAPO-34 [98-102].

Varzaneh et al [102] observed that with ZSM-5 zeolite, the ratio of propylene to ethylene (O/E) was higher at lower acidity as shown in Figure 2.8. Similarly, when SAPO-34 was used, which has strong acid sites, the ratio of P/E was smaller. They noticed that when the zirconium and cerium were added, it was noticed that the middle and strong acid sites were increased. These acids are favorable for the production of the carbenium which can increase the presence of the propylene and ethylene.

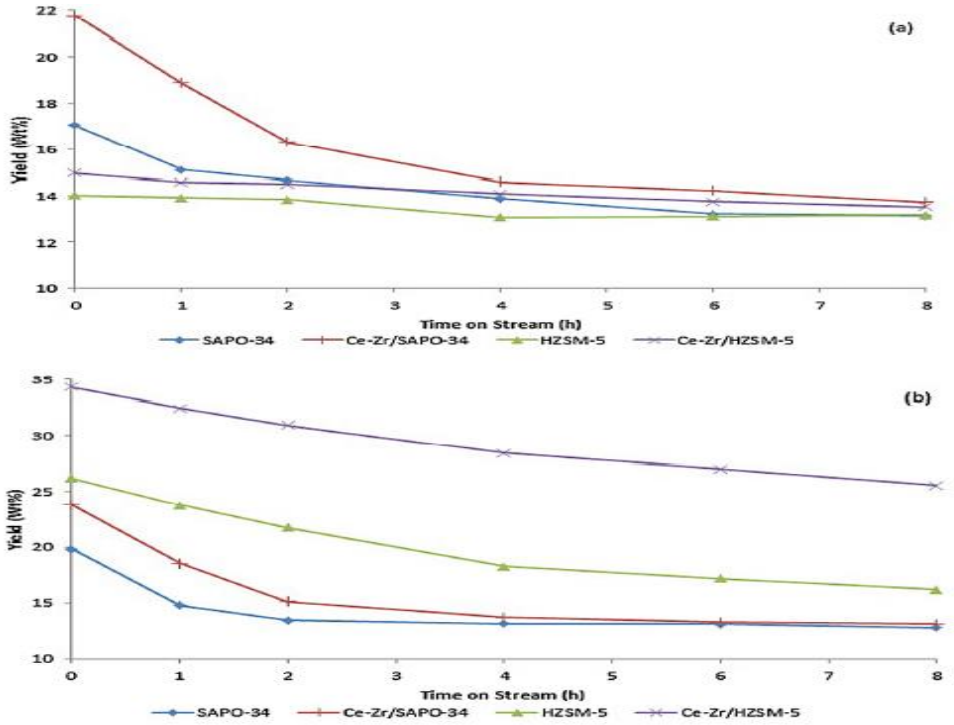

Figure 2.8: The yield of (a) ethylene and (b) propylene [102].

2.7. Characterization

2.7.1. X-ray diffraction

X-ray diffraction (XRD) is an analytical method for reliable and fast identification of the crystal phase. It can give a quantitative and qualitative analysis of solid samples and powder samples. Its electromagnetic radiation has highly energetic. Its energy is localized between γ-rays and ultraviolet (UV) radiation in the range between 200 eV and 1 MeV [103]. XRD can provide data about the crystallite orientation and its stress, crystallinity, phase identification and crystallite size. The crystal type of synthesized zeolites have to be examined to confirm the formation of the targeted zeolite. It looks like a fingerprint, in which each zeolite has its own pattern. By XRD, it will be easier to recognize whether the

product sample is amorphous or crystalline. Even it can tell whether it is pure phase or mixed phase. Additional to that, the amount of impurity can be determined roughly. Crystal size can be calculated by the famous Scherer equation [104]:

Equation 2.1: Scherer equation for crystallite size determination

$$D_p = \frac{0.9\lambda}{\beta_{1/2} \cos\theta}$$

Where λ is wavelength in Angstroms, $\beta_{1/2}$ is full width half maximum in degrees and θ in degrees.

A beam of X-rays (Rigaku Miniflex Company) was pointed on a specimen for the identification of the phase and the crystallinity of the powder samples where the X-ray needed to be impinged by scattering the crystal in all directions. The samples with the fine powder need to be replaced in a sample holder. The X-ray beam has a wavelength of 0.154184 nm with a radiation of CuKα [103]. Common scanning range of zeolitic materials is 5-50^o and the scanning speed can be varied between 0.5-3 degree per min and the result collection is at each 0.02^o.

2.7.2. Scanning electron microscopy

Zeolite morphology and crystal size of the synthesized zeolite can be found using field emission scanning electron microscopy (FE-SEM). FE-SEM can provide the morphological

information by magnifying the image of the samples and provide the chemical information from the specimen.

Samples were characterized with field emission scanning electron microscopy (LYRA 3 Dual Beam, Tescan) having a dual beam (electron and focused ion beam). It combines field emission scanning electron microscopy (FE-SEM) and a high-performance focused ion beam (FIB) system in one chamber. The system is integrated with Energy-dispersive X-ray spectroscopy (EDX) detector (Backscattered electron). Using EDX, elemental analysis of the zeolite can be characterized and the elemental compounds can be evaluated and the composition of each element can be determined through the generation of X-ray spectrum on the specimen.

Sample preparation for SEM and EDX analysis can be prepared as follows: Electron guns are used to produce a beam of electrons. This beam of electrons focuses in a specimen. The electron gun emits electrons from field-emission gun to produce the image. The FE-SEM has a resolution reach up to 1.2 nm with magnification up to 1,000,000 X.

Samples for FE-SEM can be prepared as follows: small portion of zeolite powder was added to a small amount of ethanol to prevent the formation of the overcrowding of the zeolite particles. Then a drop or two of the mixture were added to carbon tape pasted on a holder.

After evaporating the ethanol, samples were coated with a small coat of gold solution for 1 min. Samples were ready for the characterization after the coating.

2.7.3. Nuclear magnetic resonance spectroscopy

The molecular structure of the synthesized zeolite was determined using solid state Nuclear Magnetic Resonance Spectroscopy (NMR). The frameworks of zeolites are consisting of atoms connected to each other. The orientation of the atoms can be arranged in different orientation or coordination when the crystallization of the mixture happens. The main components in zeolitic materials are silica and aluminum. As a result, the coordination type of both silica and aluminum need to be determined. Usually, the coordination type of the alumina in the zeolitic framework is in a tetrahedral coordination. Sometimes this alumina became as an extra-framework by having an octahedral coordination. Similarly, in identifying the coordination type of silica. Silica usually can be coordinated in a form of tetrahedra or a multiple of tetrahedral atoms. These coordination types can be determined by the solid state ^{29}Si or ^{27}Al NMR.

2.7.4. Temperature-programmed desorption

Zeolites are solid acid materials which have two types of acid sites, namely, Lewis acid site and Brønsted acid site. Aluminum provides the Lewis acid and the proton on the framework of the zeolite provide the Brønsted acid. These acidities in total need to be calculated to study its effect on the selectivity and conversion of certain reaction. One of the most

common methods for acidity measurement is the temperature-programmed desorption (TPD). By this method the ammonia gas is being desorbed in zeolite pores.

Samples need to be degassed at high temperature with a continuous flashing of helium gas for 10 minutes to remove all impurities. The temperature was raised from room temperature to 550 ^{o}C by heating rate of 25 ^{o}C/min. After degassing, the temperature was reduced to 100 ^{o}C by cooling rate of -50 ^{o}C/min. At this time, a mixture of helium gas with ammonia gas was flowing over the sample for 300 min until the saturation of the sample. After saturating the samples with ammonia gas, the sample was heated up to 550 ^{o}C in the rate of 5 ^{o}C/min to desorb all adsorbed ammonia.

2.7.5. Nitrogen adsorption-desorption measurement

Brunauer, Emmett and Teller isotherm (BET) is an instrument used to evaluate the surface area and pore volume of powder samples. The concept of BET analyzer depends on the physisorption (physical adsorption). This kind of physical adsorption based on the weak Van der Waals attraction. This physical adsorption is characterized by the following features [105]:

1. Low adsorption heat
2. It can accommodate both monolayer and multilayer of adsorption
3. It can be operated at lower temperature
4. Enthalpy of adsorption is low (20 - 40 k.J/mole)
5. It is a reversible process

6. Rapid adsorption
7. No electron transfer

Several assumptions were considered in the BET isotherm equation. These assumptions are [105]:

1. Homogeneous surface
2. The energy of the first layer is same as the heat of adsorption
3. Second layer and higher than the second layers has energy similar to the heat of condensation
4. At infinite number of layers, it will be obtained at saturation pressure

One form of BET equation is [105]:

Equation 2.2: BET equation

$$\frac{V}{V_m} = \frac{CP}{(P_o - P)[1 + (C-1)(P/P_o)]}$$

Where

$$C = constant$$

$$P = Equilibrium\ pressure$$

$$P_o = Saturation\ pressure$$

$$V = Volume\ of\ gas\ adsorbed$$

$$V_m = Volume\ of\ monolayer\ gas\ adsorbed$$

CHAPTER 3

OBJECTIVE

Petrochemical industries are expanding due to the enlargement of the world population. The capability of the industries still limited compared to the large demand of humanity to the chemical productions. The availability of crude oil as one of the primary energy Oils are decreasing and they will continue during coming decades and oil with very long chains start to appear in some reservoirs and will appear soon in the other reservoirs. Additional to that, the costs will increase due to the decrease in the oil recovery. As a result of that, continuous researches are required in several fields such as the oil enhancement recovery, zeolite modification and the modification of reaction routes.

Catalytic cracking in the presence of solid catalysts is one of the most processes used in the petrochemical industry. Such kind of reaction needs a powerful catalyst to work in harsh conditions, for instance high pressure and high temperature. Usually, zeolite modifications can be performed with different methods as shown in Figure 3.1.

In our study, we are targeting to obtain high selectivity towards olefin. We will synthesize pure MTW zeolite with different silica to aluminum ratio. Then we will modify the pure

ZSM-12 zeolite by impregnation method. In the impregnation, lanthanum, cerium and boron will be introduced the framework of MTW zeolite. The zeolite will be evaluated in the catalytic cracking of n-hexane. Further evaluation for the hydrothermal stability of the best samples in the hot liquid water. In another kind of modification, desilication will be used in the presence of different concentration of sodium hydroxide solution to increase pore volume and surface area if the zeolite.

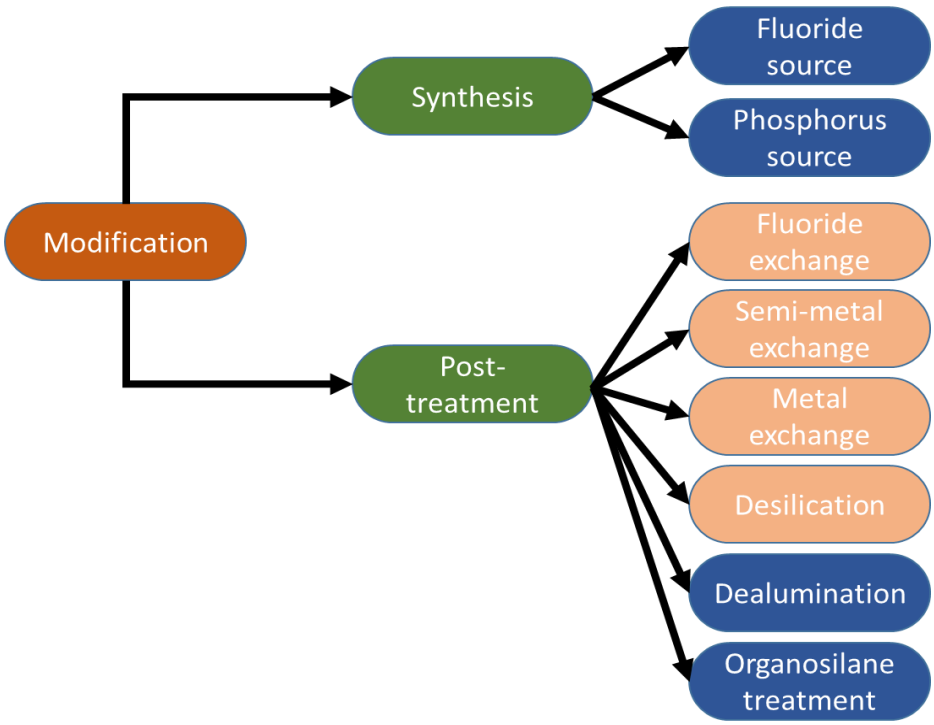

Figure 3.1:General stratigies of zeolite modifications.

CHAPTER 4

EXPERIMENTAL SYNTHESIS

4.1. Apparatus

Synthesis of ZSM-12 zeolite was performed by the hydrothermal method. Prior to the synthesis, the apparatus needed to be used in the experiments. The following apparatus was used.

1. Beakers for gathering and mixing the chemical.
2. Magnetic stirrer bars.
3. Hot plate stirrer to stir the mixture.
4. Spatula and spoon.
5. Weighing balance.
6. Graduated cylinder.
7. Teflon bottle.
8. Stainless steel autoclave.
9. Thermal oven.
10. Centrifuge for separate the product from the solution.
11. Filter paper for filtration.
12. Vacuum pump.
13. Furnace for calcination.

14. Microwave for ion exchange.

4.2. Reactants

Usually the following materials are used in the synthesis of zeolites generally and MTW zeolite particularly without further purification. In our synthesis of ZSM-12 zeolite, the following chemicals were used:

1. Aluminum sulfate octahydrate ($Al_2(SO_4)_3.18H_2O$, Sigma Aldrich) as aluminum source.
2. Colloidal silica 40% suspended in water (SiO_2,40 wt. % in water, Nissan Chemicals) as silica source
3. Sodium hydroxide (NaOH) as mineralizer agent.
4. Tetraethyl ammonium bromide (TEABr, 98%) was used as an organic structure directing agent (OSDA).
5. Deionized water.
6. Ammonium nitrate ($NH_4(NO_3)$) for ion exchange.
7. Ammonium fluoride (NH_4F) for ion exchange.
8. Boric acid (H_3BO_3) as a boron source.
9. Lanthanum nitrate hexahydrate as lanthanum source.
10. Ammonium cerium (IV) nitrate as cerium source.

4.3. Synthesis of ZSM-12 zeolite

MTW zeolite was synthesized at different Si/Al ratio. The gel mixture was containing colloidal silica (40 wt. % in water, Snowtex 40, Nissan Chemicals) and aluminum sulfate octahydrate $Al_2(SO_4)_3.18H_2O$ as silica source and aluminum source, respectively. Tetraethyl ammonium bromide (TEABr) was utilized as OSDA and sodium hydroxide was used to adjust phase purity and mineralizer agent source. The gel mixture was prepared as follows. X g of sodium hydroxide (NaOH) was added to Y g of deionized water (DI). After sodium hydroxide dissolved in DI water, Z g of aluminum sulfate octahydrate was added to the mixture followed by 5.02 g of TEABr. In another beaker, 28.47 g of colloidal silica was diluted with 11.39 g of DI water. At the end, the solution of the first beaker was added gradually to the solution in the second beaker and the whole mixture was stirred for 90 min at ambient temperature. The mixture then was transferred to a PTFE-lined stainless steel autoclaves with a volume of 100 ml and then heated in a static oven at 145 ^oC for 120 h. The typical values for X, Y and Z are 1.18, 14.05 and 0.79 g, respectively. Other values are shown in the Appendix A in Table A.1. Mixing scheme is shown in Figure 4.1.

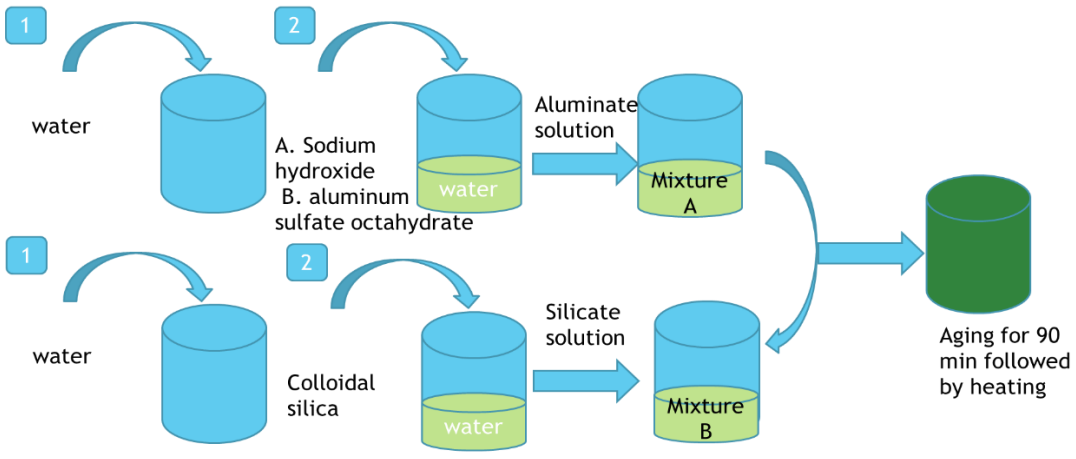

Figure 4.1: Mixing steps in the synthesis of MTW zeolite.

The molar ratio of SiO_2/Al_2O_3 in the original gel mixture for the pure MTW zeolite was designed to be in the range between 160 and 400. The typical molar ratio is 1 SiO_2:0.1235 TEABr: 0.0063 Al_2O_3: 0.0778 Na_2O: 12.57 H_2O. The molar composition of other samples is shown in Appendix A in Table A.2

Static hydrothermal synthesis was carried out at 145 ^oC for 120 h in 100 ml PTFE reactor. After 120 h, the product was washed thoroughly with DI water using centrifuge until the pH reduced to 7. The product was dried for 4 h at 105 ^oC. Organic structure-directing agent presented in the zeolites frameworks was removed by calcining the samples for 21 h under air flow. During the first 30 min, the temperature was raised from ambient temperature to 550^oC and then kept for 12 h.

4.4. Ion exchange under microwave irradiation

The calcined zeolite (Na-ZSM-12) was ion-exchanged under microwave irradiation. Two kinds of ion-exchange were performed. We used two different ammonium sources which have different properties to exchange the sodium (Na) ions. The first source is ammonium nitrate (NH_4NO_3) and the second source is ammonium fluoride (NH_4F). In ammonium nitrate, there is a possibility to exchange some OH^- groups with F^- in which hydrophobic nature can be obtained. In all cases, 1 g of zeolite was mixed with 20 g of ammonium solution. Ions were exchanged at 85 ^oC for 10 min. After first ion-exchange, the powder was centrifuged once with deionized water and

then second ion-exchange was performed again. The product was washed systematically after the second ion-exchange and then dried at 105 ^{o}C for 4 h. Finally, the samples were re-calcined at 550 ^{o}C for 5 h.

4.5. Impregnation processes

After calcination, samples were divided into two groups. A sample ion-exchanged with ammonium nitrate and another with ammonium fluoride. These samples were called T1 and T2, respectively. Each group was then divided into three parts. Each part was impregnated with different metals. We impregnated ZSM-12 zeolite with lanthanum, cerium and boron. The sources of these elements were lanthanum nitrate hexahydrate, Ammonium cerium (IV) nitrate and boric acid. The impregnation was performed with different weight percentage; 0.5, 1 and 2 wt.%. Samples impregnated with lanthanum, cerium and boron as shown in Table 4.1, 4.2 and 4.3.

Table 4.1: Impregnation weight of lanthanum.

weight of lanthanum nitrate hexahydrate (g)	MW lanthanum nitrate hexahydrate	mol of lanthanum nitrate hexahydrate	mol of La	MW of La	weight of La (g)	Zeolite weight (g)	wt%
0.0779	433.01	1.80E-04	1.80E-04	138.9	0.025	5	0.5
0.1559	433.01	3.60E-04	3.60E-04	138.9	0.05	5	1
0.3117	433.01	7.20E-04	7.20E-04	138.9	0.1	5	2

Table 4.2: Impregnation weight of cerium.

weight of Ammonium cerium(IV) nitrate (g)	MW Ammonium cerium(IV) nitrate	mol of Ammonium cerium(IV) nitrate	mol of Ce	MW of Ce	weight of Ce (g)	Zeolite weight (g)	wt%
0.0978	548.22	1.78E-04	1.78E-04	140.12	0.025	5	0.5
0.1956	548.22	3.57E-04	3.57E-04	140.12	0.05	5	1
0.3913	548.22	7.14E-04	7.14E-04	140.12	0.1	5	2

Table 4.3: Impregnation weight of boron.

weight of Boric acid (g)	MW boric acid	mol of boric acid	mol of B	MW of B	weight of B (g)	Zeolite weight (g)	wt%
0.1430	61.83	2.31E-03	2.31E-03	10.811	0.025	5	0.5
0.2860	61.83	4.62E-03	4.62E-03	10.811	0.05	5	1
0.5719	61.83	9.25E-03	9.25E-03	10.811	0.1	5	2

Impregnation weights are shown in Table 4.1, 4.2 and 4.3. The impregnation procedure was performed as follows. The metal was dissolved in 5 ml of ethanol (C_2H_5OH). Dissolving these compounds were easy at ambient temperature except boric acid, which required heating source. It was dissolved at 75 ^oC. After dissolving these metals in ethanol, zeolite samples were added to the solution and mixed gently to assure the uniform distribution of the solution on the zeolite samples. Impregnation steps are shown in Figure 4.2. Samples were allowed to dry at ambient temperature. After that, samples were calcined at 550 ^oC for 5 h.

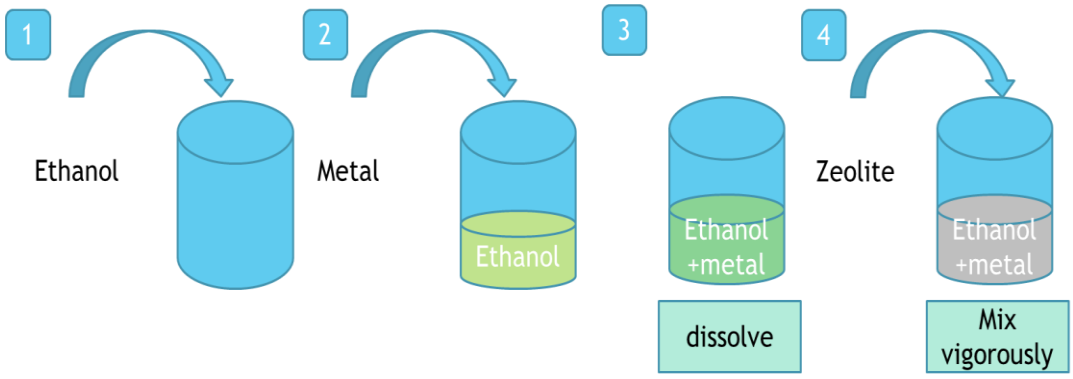

Figure 4.2: Impregnation steps in ZSM-12 zeolite.

4.6. Alkaline treatment under microwave irradiation

Hierarchical MTW zeolite was treated in the presence of basic solution. The post treatment was operated under microwave irradiation. Three different zeolite samples were used in the study. These samples have different silica to aluminium (Si/Al) ratio. The initial gel mixture of these samples have the following Si/Al ratio; 80, 140 and 200. A solution of 0.1 M sodium hydroxide was prepared. One gram of H-ZSM-12 zeolite was added to each 20 g of sodium hydroxide solution. Treatment was operated under microwave irradiation at 85°C for 10 min. After treatment, samples were washed systematically with DI water and the pH was brought down to 7. After drying at 105 ^{o}C, samples were re-calcined at 550 ^{o}C for 12 h. Then samples were ion exchanged with 2 M solution of ammonium nitrate and then re-calcined with same procedure mentioned above.

4.7. Zeolite characterization

Zeolite samples were characterized with different instrumental techniques to study the physical and chemical properties of the samples. X-ray diffractometric instrument (XRD) with CuKα radiation in the period of $2\theta = 5^{o}$ to 50^{o} was used for phase identification. The scanning speed was 3^{o} per min with scanning step of 0.02. Field-emission scanning electronic microscopy (FE-SEM, LYRA 3 Dual Beam from Tescan Company) was used for particle size and crystal morphology identification. Temperature-programmed desorption (TPD) was used for the identification of the

acid sites. Solid-state ^{27}Al and ^{29}Si NMR spectra was used to identify the coordination of both silica and aluminum. The isotherms of nitrogen adsorption were measured using liquid nitrogen N_2 by a porosimeter analyzer (BELsorp mini, BEL Japan) at 77 K. The samples were degassed at 300 ^{o}C in vacuum under ambient atmosphere before the measurement for 12 h. Brunauer, Emmett and Teller (BET) isotherm was applied for determining the total surface area.

4.8. Catalytic testing

MTW zeolite was modified with different methods. These modification methods were desilication and impregnation. The performance of modified MTW zeolite was evaluated by the cracking of n-hexane in a fixed-bed flow reactor system. Modified MTW zeolite samples were pelletized in 300 micron and then 0.8 g of modified zeolite was packed in a haste alloy reactor tube of 10 mm ID. Then the bed was supported by a layer of inert alumina balls of 1 mm diameter. The cracking of n-hexane was performed at 650 ^{o}C (923 K) in the presence of nitrogen flow of 25 ml/min. The weight hourly space velocity (WHSV) was fixed to be 3.6 h^{-1}. The reaction products were analyzed by gas chromatography (GC). Gaseous reaction products were analyzed in a refinery gas analyzer (Agilent) equipped with FID and TCD detectors. The liquid products were analyzed for their hydrocarbon content in a GC PONA analyzer. The analytical results were combined to calculate the conversion and olefins yields.

4.9. Stability tests

The stability test of the parent and zeolite samples were studied. The method of this test is as follows. Deionized water (30 g) was poured to 0.2 g of zeolite sample and mixed together in an autoclave. The sample were heated at 200 ^{o}C for 72 h. The sample was cooled and then centrifuged to separate the powder from the water. The phase of the sample was tested using XRD to check the crystallinity of the sample. Usually a reduction in the crystallinity will happens. The change in the acidity was determined by TPD to compare it with the sample before the treatment.

CHAPTER 5

SYNTHESIS OF ZSM-12 ZEOLITE

5.1. Introduction

Zeolites importance encouraged many scientist to modify the synthesis factors of many types of zeolites. This attention to zeolites modifications is due to the zeolitic nature in adsorbing the hydrocarbon molecules [106]. One of the most important zeolite is ZSM-12 (MTW) zeolite which was developed for the first time by Mobil Research and Development scientists [16-18]. ZSM-12 zeolite has 12 member-rings (MR) and one dimensional pore system which was determined by LaPierre and coworkers [19]. Its pore size is slightly larger than MFI zeolite. Its pore size is 0.56 x 0.61 nm. This pore size, made ZSM-12 zeolite to be proper long hydrocarbon molecules [15].

Usually, ZSM-12 zeolite synthesis in the presence of sodium aluminum oxide. However, in our experiments, we utilized the aluminum sulfate octahydrate to be used as an Al source [15, 107, 108]. The synthesis of ZSM-12 zeolite cannot be synthesized unless organic structure directing agents (OSDA) added to synthesis mixture. The template source can affect the morphology of the produced zeolite. As an example, the morphology using methyl trimethyl ammonium bromide (MTEABr) as OSDA is rice-shape crystal. However,

the morphology was spherical in the presence of ethyl ammonium bromide (TEABr) and tetra ethyl ammonium hydroxide (TEAOH) as OSDA [66, 78]. As an example, the morphology was spherical when the template was tetraethylammonium bromide and tetraethylammonium hydroxide as shown in Figure 5.1.

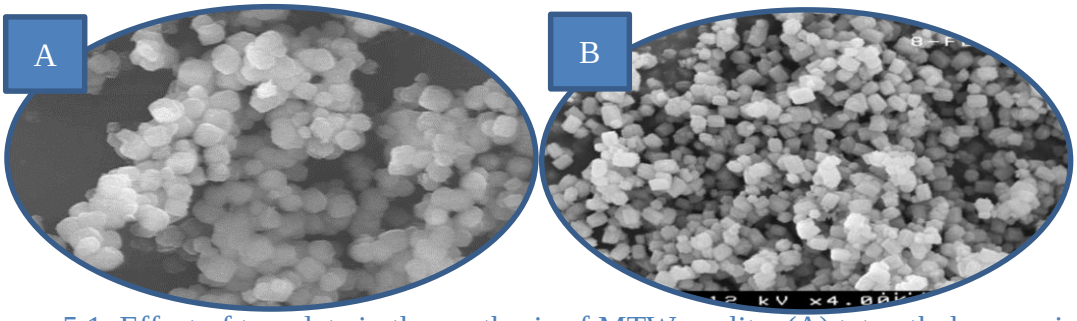

Figure 5.1: Effect of template in the synthesis of MTW zeolite, (A) tetraethylammonium bromide, (B) tetraethylammonium hydroxide.

Similarly, the morphology can be changed to rice-shaped crystal or needle-shaped crystal if the template used was methyl trimethyl ammonium bromide (MTEABr) or benzyltrimethylammonium chloride (BTMACl), respectively as shown in Figure 5.2.

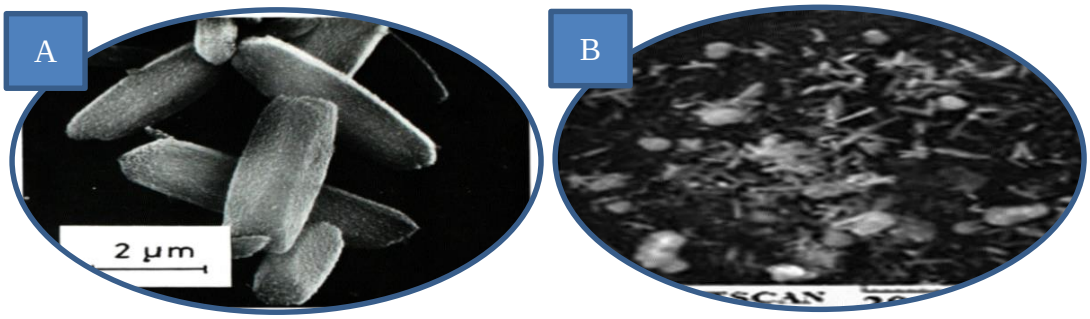

Figure 5.2: Effect of template in the synthesis of MTW zeolite, (A) methyl trimethyl ammonium bromide, (B) benzyltrimethylammonium chloride.

In all cases, template can also affect the synthesis time, the synthesis temperature and crystal size as shown in Table 5.1.

Table 5.1: Effect of template in the synthesis time and crydtal size.

Author name	Template	Synthesis temperature (oC)	Synthesis time (day)	Crystal size	Ref
Gopal et al	TEAOH	160	5.5 days	1 μm	(Gopal et al. 2001)
Yoo et al	TEABr	160	5 days	1 μm	(Yoo et al. 2003)
Xuefeng et al	TEABr	160	5 days	1 μm	(Bai et al. 2009)
L. Dimitrov et al	TEAOH	160	6 days	1.5 μm	(Dimitrov et al. 2011)
S. Mehla et al	BTMACl	160	6 days	10 μm	(Mehla et al. 2013)
Ernst et al	MTEABr	160	8.5 days	4 μm	(Ernst et al. 1987)
Chokkalingam et al	TEABr	100	90 days	6 μm	(Chokkalingam et al. 2013)
Chokkalingam et al	MTEABr	150	10 days	6 μm	(Chokkalingam et al. 2013)

In this study, Different Si/Al ratios were used to synthesize pure ZSM-12 zeolite in the presence of TEABr as the cheapest OSDA. Additionally, alkalinity concentration and the temperature of the synthesis were varied to obtain pure ZSM-12 zeolite.

5.2. Results and discussion

5.2.1. Synthesis of ZSM-12 zeolite with different SiO_2/Al_2O_3 ratio

Synthesis of ZSM-12 zeolite was performed using different silica to alumina (SiO_2/Al_2O_3) ratio. These ratios were 160, 240, 320, 360 and 400. Since the source of chemicals can affect the on the produced zeolite. We tried to fix all sources of all chemicals. In all of these

experiments, the aluminum source was aluminum sulfate octahydrate. The silica source and alkalinity sources were colloidal silica and sodium hydroxide, respectively. Samples were characterized using XRD to identify phase patterns of the produced zeolites. As shown in Figure 5.3, ZSM-12 (MTW) zeolite was produced in all samples at 145 ^{o}C with different ratio. We were not able to produce ZSM-12 zeolite with SiO_2/Al_2O_3 ratio of 80 at our condition and the XRD results were shown to be amorphous. However, at the constant alkaline condition, we noticed that the phase is getting some minor impurities by varying the SiO_2/Al_2O_3 ratio. At the SiO_2/Al_2O_3 ratio of 160, we noticed a small impurities (less than 2%) of ZSM-5 was observed. Increasing the SiO_2/Al_2O_3 ratio to 240, led to the removal of this impurity. Further increase in the ratio to 160 and 180 led to the formation of small percentage from cristobalite phase. This cristobalite was then removed totally by a further increase in the SiO_2/Al_2O_3 ratio up to 400. Our notification was as follow:

1. ZSM-12 zeolite is affected to the ZSM-5 zeolite at lower Si/Al ratio
2. At certain Si/Al ratio, the presence of ZSM-5 zeolite phase disappears
3. Further increase in the Si/Al ratio led to the formation of cristobalite
4. Further increase of the Si/Al ratio, led to the disappearance of the cristobalite

Further experiment is required to identify whether another kind of impurities will appear or not. Another factor effect the phase purity is the crystallization rate. For cristobalite phase, we and other noticed that it can be removed by either decreasing the synthesis time, synthesis temperature or alkalinity insignificantly [66]. Reducing the Al content, lead to the increase of Si content in the zeolite framework. This increase in the silica amount enhanced

the crystallization rate of ZSM-12. This was also noticed by Ernst et al in the presence of methyl triethyl ammonium bromide (MTEABr) as OSDA [66].

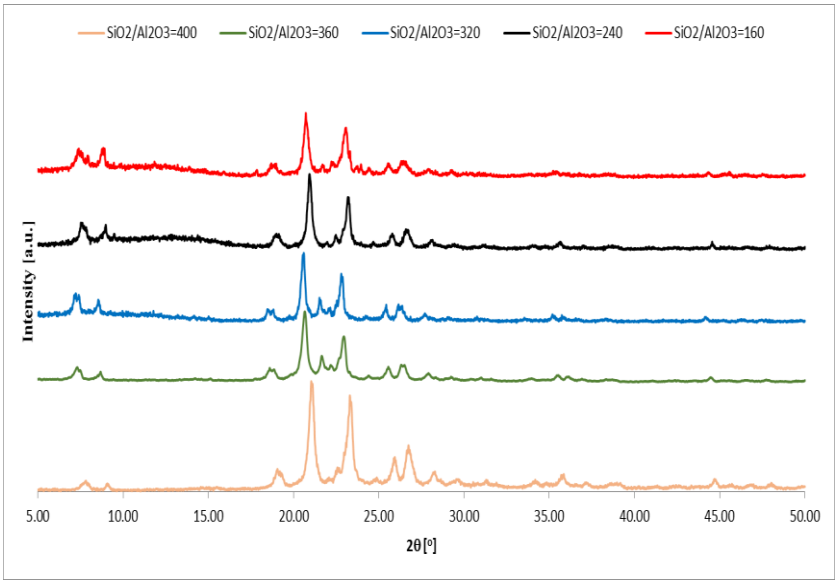

Figure 5.3: XRD patterns of ZSM-12 zeolite synthesis at different SiO_2/Al_2O_3.

FE-SEM micrographs of ZSM-12 zeolite samples are shown in Figure 5.4. In all samples, agglomeration was shown and the crystal shapes were irregular in when the ratio were between 160 and 240 with average agglomerates of 2 and 1.8 μm respectively. Two kind of morphologies were observed at SiO_2/Al_2O_3 ratios of 320 and 360. The morphologies were hexagonal crystal and cubic shaped-agglomerates. The crystal size of the cubic particle was 1.6 and 1 micrometer, respectively. The morphology of MTW zeolite can be cubic, spherical, needle, rice-shaped crystals and bundles of hexagonal platelets as reported by Lai et al [109].

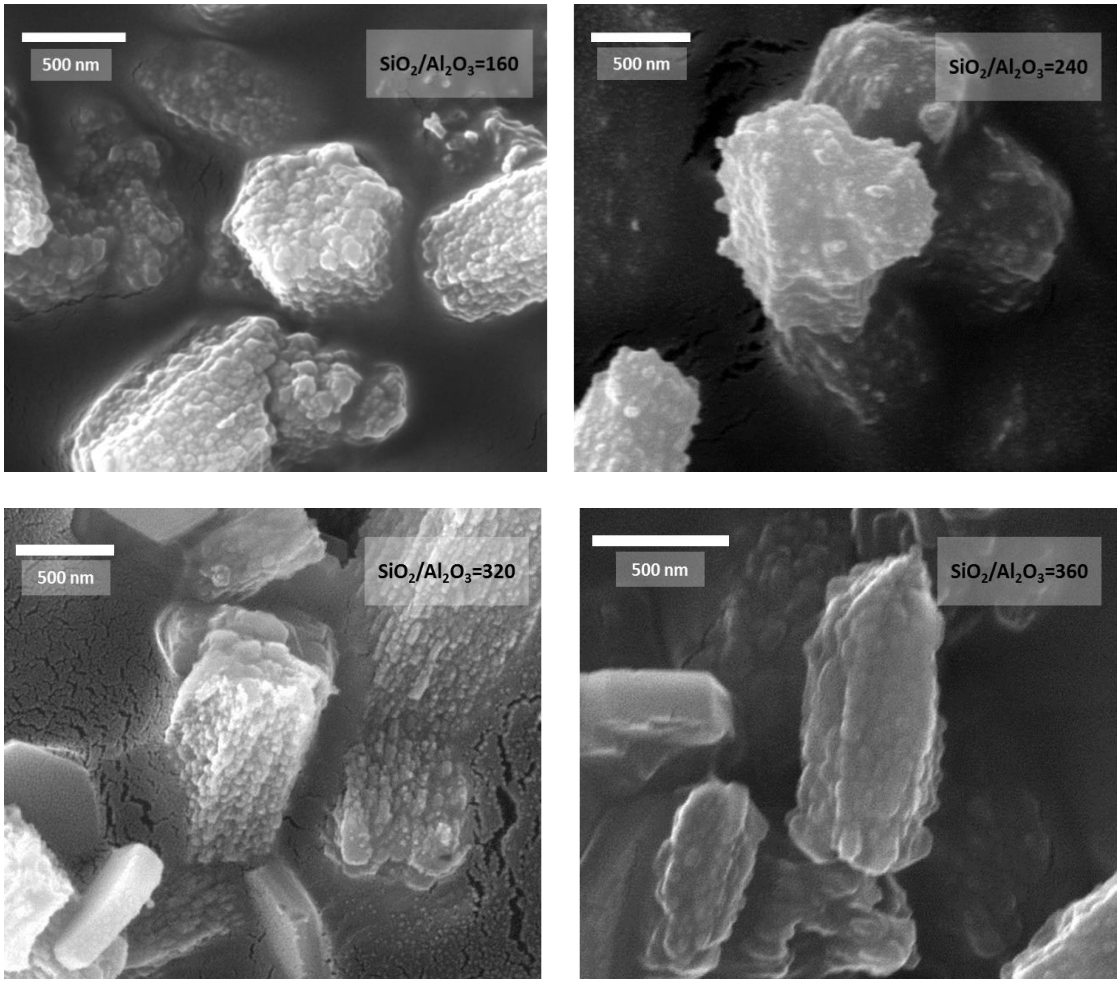

Figure 5.4: FE-SEM results of different SiO_2/Al_2O_3.

5.2.2. Effect of alkalinity in the purity of ZSM-12 zeolite

Obtaining the pure phase of ZSM-12 zeolite is a challenging issue because of the narrow synthesis window. Tuning the synthesis parameters such as alkalinity can lead to either increase or decrease of the impurities. To localize the range of pure ZSM-12 zeolite synthesis, MTW zeolite need to be synthesized with different alkalinity concentration at each silica to aluminum ratio (Si/Al). In our studies, we studied the alkalinity at 140 ^oC to produce pure ZSM-12 zeolite at different Si/Al ratio ranged between 40 and 250. At SiO_2/Al_2O_3 of 80, we found that the ZSM-12 zeolite cannot be produced even by varying the alkalinity ratio ($NaOH/SiO_2$) between 0.144 and 0.156. In this range, produced material

was a mixture of amorphous material and starting crystallization of ZSM-5 (MFI) zeolite. XRD patterns are shown in Figure 5.5.

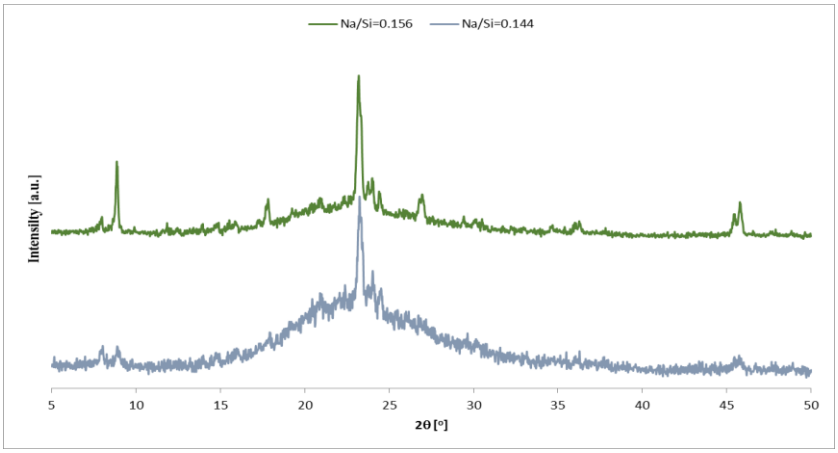

Figure 5.5: XRD patterns of ZSM-12 zeolite synthesized at SiO_2/Al_2O_3 of 80 with different $NaOH/SiO_2$.

At SiO_2/Al_2O_3 of 160, we found that the alkalinity can be tuned to obtain pure ZSM-12 zeolite. However, at $NaOH/SiO_2$ ratio ranged between 0.141 and 0.156. We observed that the zeolite phases in the alkalinity range of 0.141 and 0.150 were mostly ZSM-12 zeolite with minority less than 5% of ZSM-5 zeolite. All products were tested using XRD as shown in Figure 5.6.

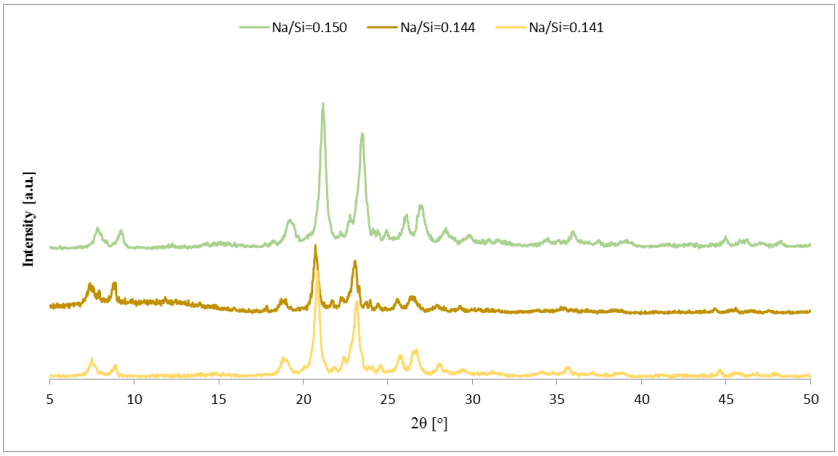

Figure 5.6: XRD patterns of ZSM-12 zeolite synthesized at SiO_2/Al_2O_3 of 160 with $NaOH/SiO_2$ variation in the range between 0.141 and 0.150.

However, additional increase in the ratio of alkalinity to 0.156 led to the total removal of all impurities as shown in the XRD pattern in Figure 5.7.

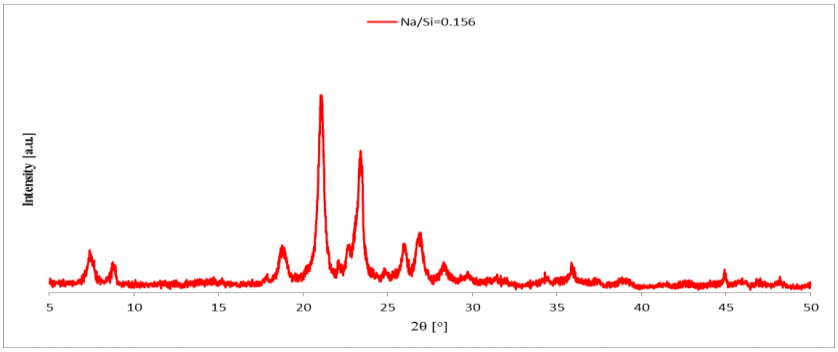

Figure 5.7: XRD pattern of ZSM-12 zeolite synthesized at SiO_2/Al_2O_3 of 160 and $NaOH/SiO_2$ of 0.156.

Pure ZSM-12 zeolite was produced at SiO_2/Al_2O_3 of 280 and $NaOH/SiO_2$ ratio of 0.150 as shown in Figure 5.8.

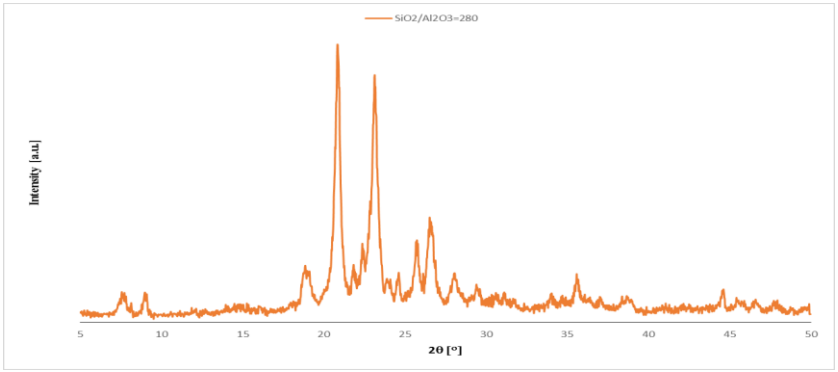

Figure 5.8: XRD pattern of ZSM-12 zeolite synthesized at SiO_2/Al_2O_3 of 280 with $NaOH/SiO_2$ of 0.150.

In the SiO_2/Al_2O_3 ratio of 320, the alkalinity ($NaOH/SiO_2$) ratio was varied between 0.137 and 0.156. It was observed that at when the alkalinity ratio varied in the range between 0.132 and 0.137, ZSM-12 zeolite was produced as a minor phase as shown in Figure 5.9.

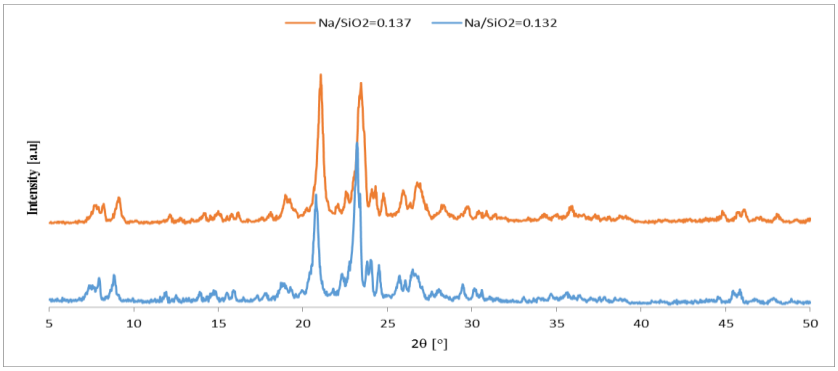

Figure 5.9: XRD patterns of ZSM-12 zeolite synthesized at SiO_2/Al_2O_3 of 320 with $NaOH/SiO_2$ variation in the range between 0.132 and 0.137.

An additional increase in the ratio of alkalinity between 0.144 and 0.156, we found that both ZSM-5 zeolite and cristobalite was produced as a minor phase as shown in the XRD patterns in Figure 5.10.

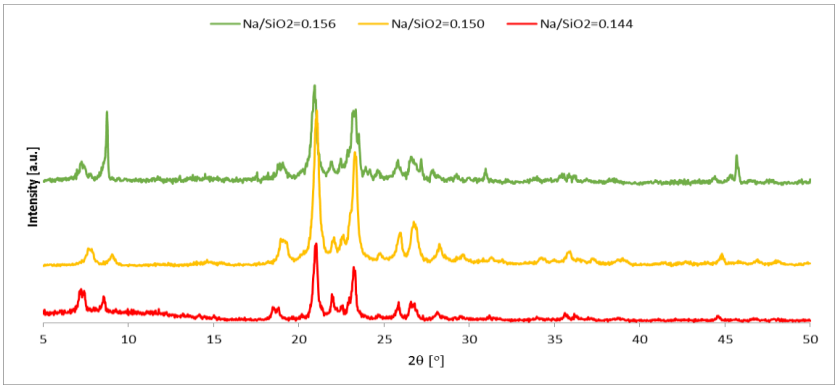

Figure 5.10: XRD patterns of ZSM-12 zeolite synthesized at SiO_2/Al_2O_3 of 320 with $NaOH/SiO_2$ variation in the range between 0.144 and 0.156.

At SiO_2/Al_2O_3 of 400, pure ZSM-12 zeolite was produced at $NaOH/SiO_2$ ratio of 0.144. The XRD pattern was shown in Figure 5.11.

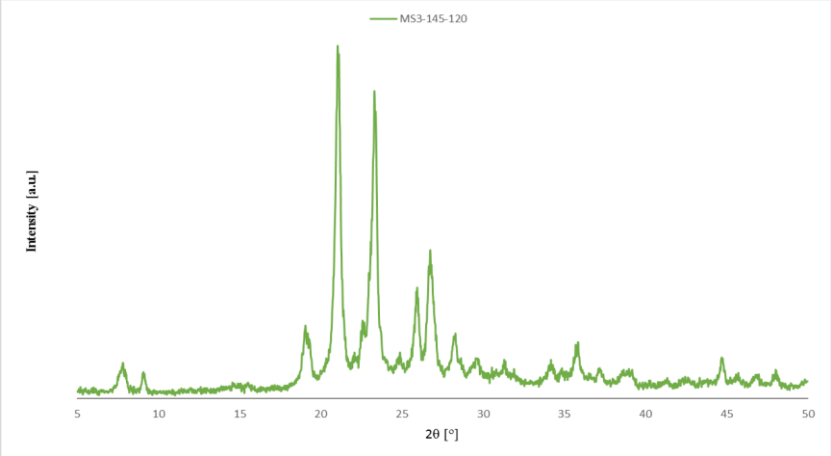

Figure 5.11: XRD pattern of ZSM-12 zeolite synthesized at SiO_2/Al_2O_3 of 400 with $NaOH/SiO_2$ of 0.144.

5.2.3. Effect of temperature on the synthesis of ZSM-12

ZSM-12 zeolite is too affected by the synthesis temperature. It was shown that the ZSM-12 zeolite can be synthesized at different temperature, but with manipulating the other parameters specially the synthesis time and alkalinity concentration. As an example, synthesizing ZSM-12 zeolite with SiO_2/Al_2O_3 of 320 at 160 ^oC led to the formation of high percentage of ZSM-5 zeolite. However, reducing the temperature to 135 ^oC led to the total removal of the cristobalite and the phase was pure ZSM-12 zeolite. ZRD patterns are shown in Figure 5.12.

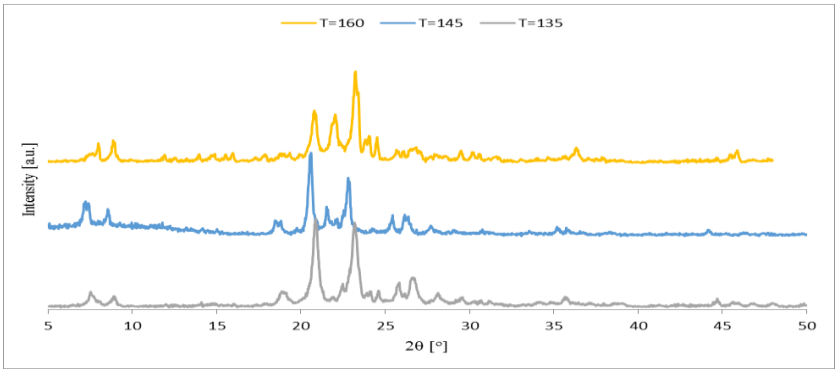

Figure 5.12: XRD patterns of ZSM-12 zeolite synthesized at SiO_2/Al_2O_3 of 320 with $NaOH/SiO_2$ of 0.144 at different temperature.

When the silica to aluminum ratio was varied, then the concentration of aluminum is changed. Changing the silica to aluminum ratio led to the change in the alkalinity concentration due to the variation in the pH of the solution. As a result, further tuning of the parameters such as alkalinity, synthesis temperature and synthesis time.

CHAPTER 6

POST-TREATMENT OF PURE ZSM-12 ZEOLITE

6.1. Introduction

Zeolite modification can be obtained by several methods. One of these methods is post-treatment. In this technique, zeolite will be synthesized without any modifications. Then after synthesis, zeolite can be modified by several methods such as desilication, dealumination, fluoride addition and impregnation with metals and semi metals. These modifications can modify both external and internal surface area, pore volume, distribution of both Lewis and Brønsted acid sites and enhance the physical properties of the zeolite.

6.2. Result and discussion

6.2.1. Effect of alkaline treatment 'Desilication' on ZSM-12 zeolite

H-ZSM-12 zeolite was treated with different concentration of sodium hydroxide (NaOH) solution under microwave irradiation (MAHyS). Treatments under MAHyS offer shorter treatment time compared to the conventional method. ZSM-12 zeolite was treated with 0.1, 0.2 and 0.3 M with time duration of 5 and 10 min. Crystal phases identified using X-ray diffraction (XRD). All peaks of H-ZSM-12 zeolite

were preserved as shown in Figure 6.1. Using BET, the surface area and pore volume of the zeolites prior to and after treatment.

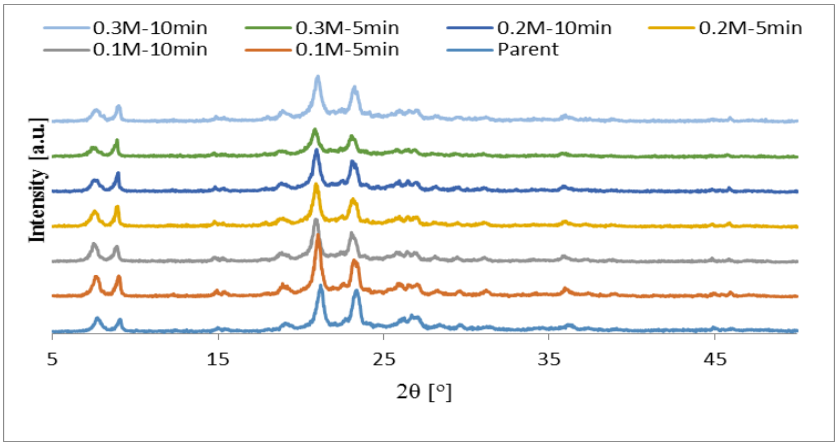

Figure 6.1: XRD patterns of ZSM-12 zeolite synthesized at SiO_2/Al_2O_3 of 160 desilicated with different concentration of alkaline solution.

The total pore volume of the parent zeolite and treated samples were evaluated using BET. As shown in Table 6.1, the specific surface area was decreased as the treatment time and concentration were increased. At specific treatment time and concentration, the specific area started again to increase. The reason behind this decreases, then re-increases is that some of the removed atoms were participated into the surface of the internal and external pore. This can be also noticed from the BET surface area. Pore volume of the parent and treated ZSM-12 zeolite are shown in Table 6.1. It was noticed that the micropores was gradually decreased from 0.175 to 0 cm^3g^{-1} as the treatment concentration increased. As shown, the treatment with 0.2 M for 10 min and harsher condition led to the total removal of all micropores. At the same time, mesopores volume was increased as the treatment time and concentration have been increased. As a result, at harsher conditions, zeolites with only mesopores were obtained. In low and moderated alkaline treatment for a short treatment time, led to

the formation of hierarchical structure where both micropores and mesoporses were presented in the zeolite samples.

Table 6.1: Surface area and pore volume of ZSM-12 zeolite prior to and after alkaline treatment. [a]t-plot, [b](p/p0=0.980), [c]$V_{meso}=V_{total}-V_{micro}$.

	S_S [a] (t-plot)	S_{BET}	S_{ext} [a] (t-plot)	V_{total} [b]	V_{micro}	V^{d}_{meso}
parent	455	306	40	0.266	0.175	0.09
0.1M-5min	121	104	83	0.228	0.053	0.17
0.1M-10min	125	112	122	0.257	0.018	0.24
0.2M-5min	134	128	160	0.329	0.021	0.31
0.2M-10min	139	134	205	0.341	0.000	0.34
0.3M-5min	165	169	437	0.528	0.000	0.53
0.3M-10min	178	180	380	0.534	0.000	0.53

Pore volume distribution was expanded over a wider range as the alkaline concentration was increased as shown in Figure 6.2

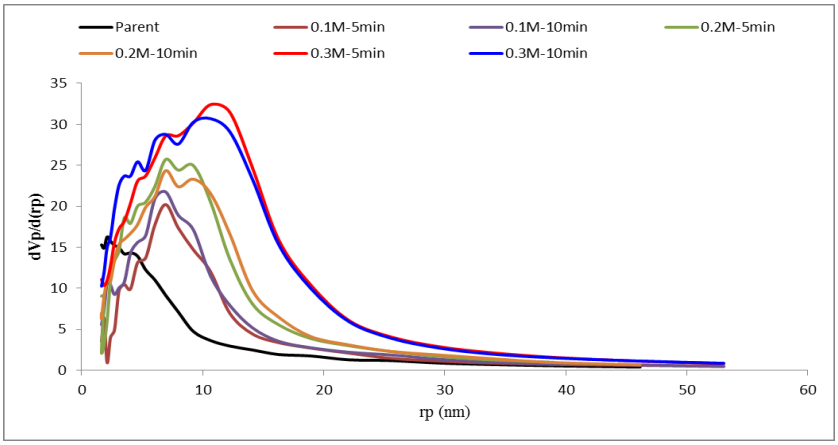

Figure 6.2: Pore volume distribution of ZSM-12 zeolite synthesized at SiO_2/Al_2O_3 of 160 desilicated with different concentration of alkaline solution.

BET isotherms were also evaluated as shown in Figure 6.3. It was noticed that the uptake was reduced to the minimum when samples was treated with 0.1 M solution. However, this uptake increased further as increasing the treatment concentration and time, but not up to the parent zeolite. It was also noticed that samples treated with harsher condition started to show the second layer of adsorption.

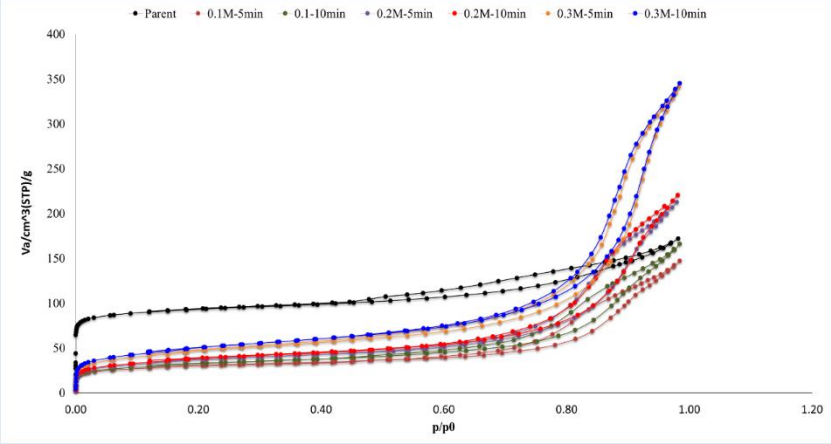

Figure 6.3: BET isotherm of ZSM-12 zeolite synthesized at SiO_2/Al_2O_3 of 160 desilicated with different concentration of alkaline solution.

Solid-state ^{27}Al and ^{29}Si NMR spectra were used for the determination of the chemical properties of the zeolite samples. In ^{27}Al NMR, it was noticed that all peaks which are shown around 55 ppm are representing the tetrahedral coordinate of aluminium as shown in Figure 6.4a. However, in ^{29}Si NMR, there is one peak around -112 ppm which is related to the tetrahedral coordinate of silica. On the other hand, on the treated samples, there is an additional peak around -108 ppm. These two positions belong to the silanol groups as shown in Figure 6.4b.

(A)

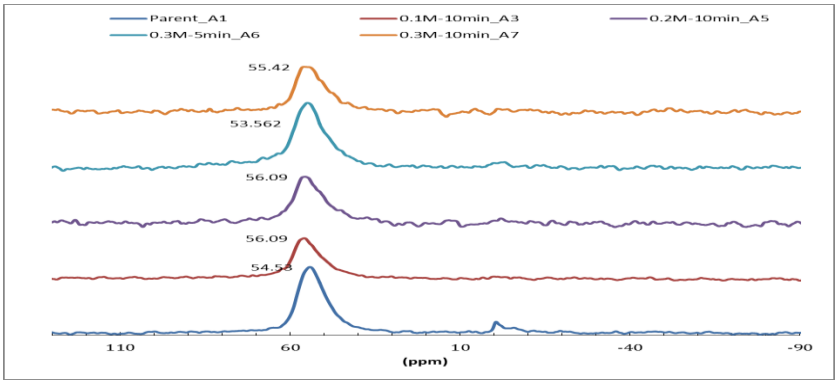

(B)

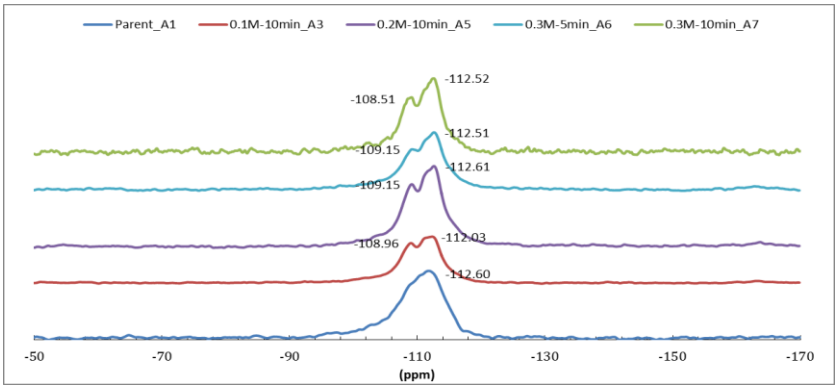

Figure 6.4: Solid state NMR of ZSM-12 zeolite synthesized at SiO_2/Al_2O_3 of 160 desilicated with different concentration of alkaline solution, (A) ^{27}Al NMR, (B) ^{29}Si NMR.

Acid sites of H-ZSM-12 zeolite prior to and after alkaline treatment was determined using temperature-programmed desorption (TPD). It was noticed that both weak and strong acid sites were observed as shown in Figure 6.5. One of these peaks appeared at low temperature and the other at high temperature around 380 and 680 K, respectively. The weak acid sites decreased as the treatment concentration increased. However, for harsher condition, the intensity of weak acid sites started to increase again. This is due to the destruction of aluminium ions and so partial dealumination was happened.

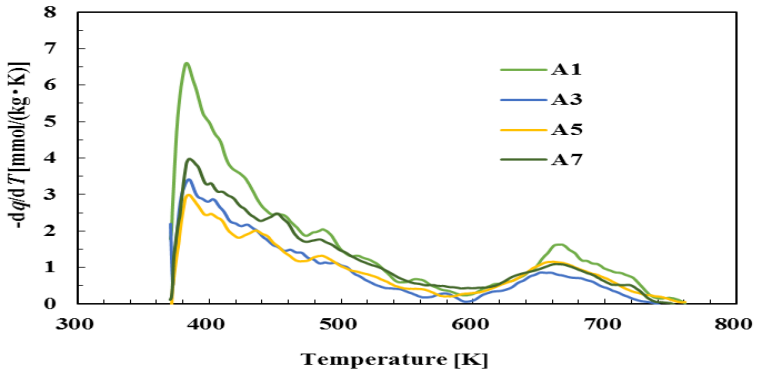

Figure 6.5: TPD of ZSM-12 zeolite synthesized at SiO_2/Al_2O_3 of 160 desilicated with different concentration of alkaline solution.

6.2.2. Ion exchange with fluoride media

Zeolite usually can be synthesized in the presence of alkaline solution. In this case, zeolite will be in the form of cation-zeolite where cation can be sodium (Na), potassium (K) or lithium (Li). This form of zeolite can't be used in the reaction due to the lack of proton in the zeolite. As a result, zeolite need to be exchanged with ammonium nitrate to get the H-zeolite form after calcination. Due to the fact that fluoride media can add a valuable hydrophobic nature to the zeolite, we proposed that the ion-exchange with ammonium fluoride instead of ammonium nitrate can enhance the presence of fluorine ions in the framework beside the exchange of the cations (Na, K or Li) with H. This fluorine ion can add the nature of the hydrophobicity to the zeolite. In our experiments, Na-ZSM-12 zeolite was exchanged with 2 M of ammonium fluoride under microwave irradiation. The ion-exchanges were performed at 85 ^{o}C for 10 min with aging speed of 500 rpm. The product was compared to both Na-ZSM-12 zeolite and H-ZSM-12 zeolite which was exchanged in the presence of ammonium nitrate. XRD patterns were preserved as shown in Figure 6.6. From XRD patterns, the crystallinity increased when Na-ZSM-12 zeolite exchanged to H-ZSM-12 zeolite. The crystallinity of Na-ZSM-12 zeolite was 100% and it was 134.65% when it was exchanged with ammonium nitrate. However, the crystallinity was further increased to 175.51% by exchanging Na-ZSM-12 zeolite with ammonium fluoride.

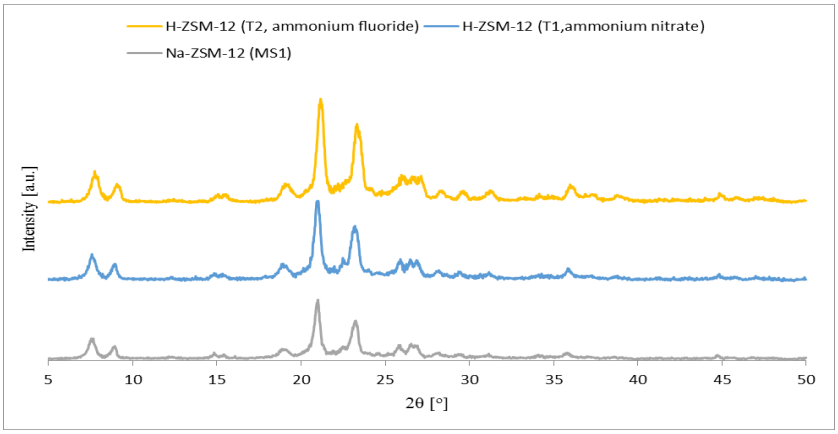

Figure 6.6: XRD patterns of ZSM-12 zeolite prior to and after ion-exchange with two different ammonium sources.

6.2.3. Impregnation

Impregnating zeolite with extra elements or compounds is a target to adjust the zeolitic properties. It can enhance the stability or the activity of the zeolites. In our studies, several ZSM-12 samples were prepared using the hydrothermal method and then samples were calcined followed by the ion-exchange to form H-ZSM-12 zeolite. Samples then dried and impregnated after the second calcination. In impregnation, we select lanthanum, cerium, boric acid and further treatment for some samples with ammonium fluoride.

Na-ZSM-12 zeolite was ion-exchanged with two different sources of ammonium products. These sources are ammonium nitrate and ammonium fluoride. Specified quantity of the metal was dissolved in ethanol, then specified quantity of H-ZSM-12 zeolite was added to the solution. The mixture was agitated gently and then the sample was allowed to dry at ambient temperature. After drying, samples were calcined at 550 ^{o}C for 5 h.

Using lanthanum, we impregnated ZSM-12 zeolite up to 2 wt. %. The crystallinity and crystal phase were reserved as shown in Figure 6.7. We found that the height of the main peak which is located around 2θ of 21 was 527 a.u. However, when the impregnation of lanthanum raised to 0.5 wt. %, we observed a reduction in the intensity of this peak to 486 a.u. with crystallinity of 96.31%. Further increase in lanthanum impregnation to 1.0% and 2% led to the reduction of the intensity of this peak in 450 and 361, respectively. The crystallinity was found to be 85.33% and 74.18% for 1.0 and 2 wt. % impregnation.

H-ZSM-12 zeolite exchanged with ammonium fluoride was impregnated with 2 wt. % of lanthanum. As shown in Figure 6.8, the XRD pattern was preserved and the intensity of H-ZSM-12 zeolite exchanged with ammonium fluoride was 682 a.u. By lanthanum impregnation, the height of this peak was reduced to 481 and the crystallinity was reduced to 68.30%. Comparing to the sample exchanged with ammonium nitrate and impregnated by 2 wt.% of lanthanum, we observed that the loss in the crystallinity is less when the zeolite exchanges with ammonium fluoride.

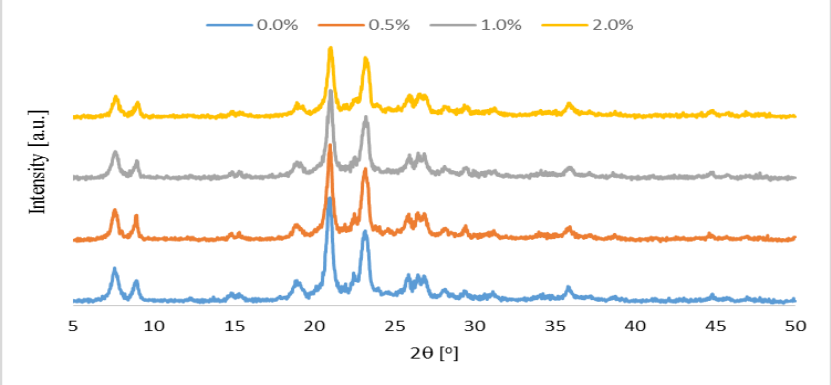

Figure 6.7: XRD patterns of ZSM-12 zeolite exchanged with ammonium nitrate prior to and after lanthanum impregnation with different load.

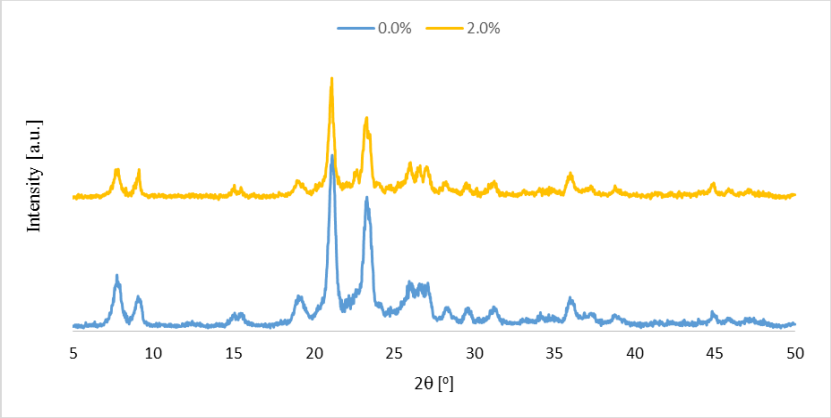

Figure 6.8: XRD patterns of ZSM-12 zeolite exchanged with ammonium fluoride prior to and after lanthanum impregnation.

Field emission scanning electron microscopy (FE-SEM) was utilized to evaluate the crystal size and the morphology of the parent H-ZSM-12 and the treated with lanthanum impregnation. We observed that the average crystal size of H-ZSM-12 zeolite was 800 nm. However, these particles are agglomerated and each particle composes of many nano particles with an average size of 80 nm as shown in Figure 6.9.

Similarly, as shown in Figure 6.10, samples exchanged with ammonium fluoride do not have an impact on the crystal size and morphology rather than producing H-ZSM-12 zeolite having some of fluorine ions in the framework.

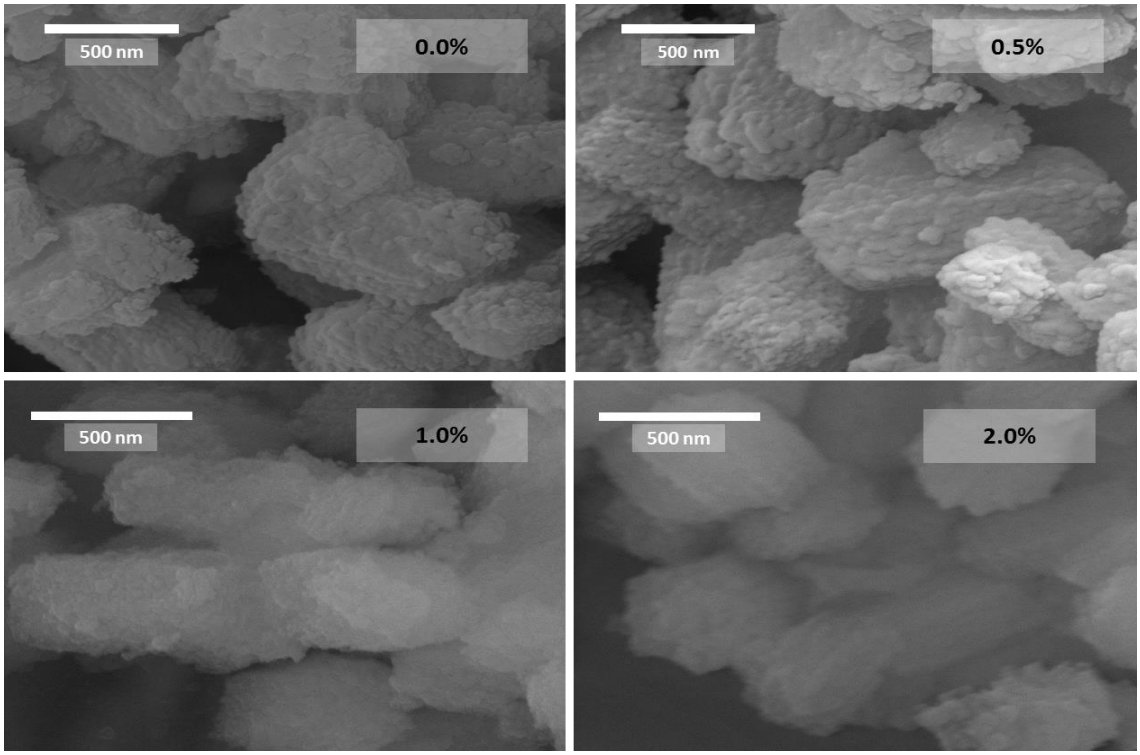

Figure 6.9: FE-SEM micrographs of impregnated ZSM-12 zeolite exchanged with ammonium nitrate prior to and after lanthanum impregnation with different load.

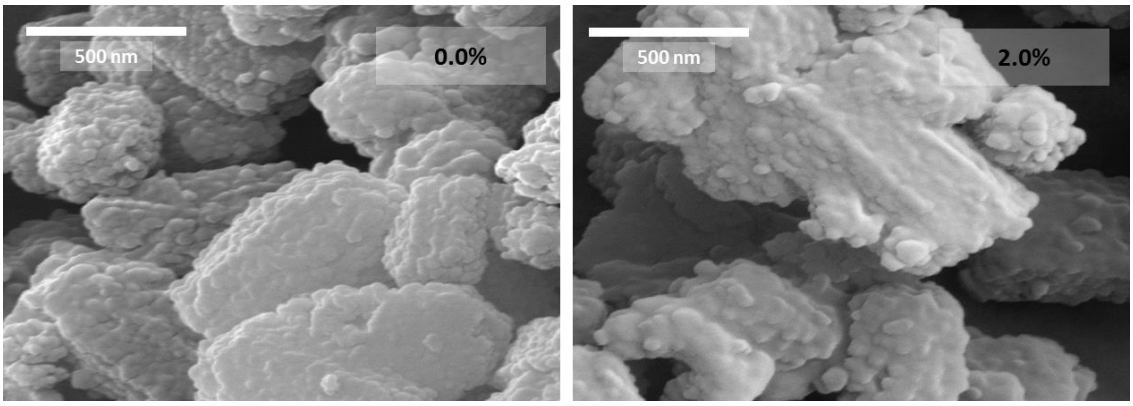

Figure 6.10: FE-SEM micrographs of impregnated ZSM-12 zeolite exchanged with ammonium fluoride prior to and after lanthanum impregnation with 2.0 wt. %.

To confirm the presence of lanthanum, we used EDX to determine the chemical composition of each sample as shown in Table 6.2. In the mixing procedure, the proposed Si/Al ratio was equivalent to 80. However, not all silica and aluminum that were available in the mixture were reacted. Some of these ions were presented as an excess and the

quantities of both silica and aluminum in the final product was around 35.72. Chemical composition of the samples which impregnated with lanthanum with different concentration were found to be 0.19, 0.43 and 0.63 wt. %, respectively.

Table 6.2: Chemical composition of H-ZSM-12 zeolite exchanged with ammonium nitrate impregnated with different load of lanthanum.

Sample name	*wt. %*				
	O	Al	Si	La	Si/Al
T1	68.42	0.86	30.72	0.00	35.72
T6	59.61	0.70	39.50	0.19	56.26
T7	57.73	0.71	41.13	0.43	58.21
T8	67.15	0.48	31.73	0.63	66.10

Chemical composition for H-ZSM-12 zeolite exchanged with ammonium fluoride was determined with EDX. It was found that the fluorine ion was present in the tested samples with 6.0%. However, further modification by lanthanum impregnation was prepared and EDX characterization was shown both fluorine and lanthanum ions in the samples as shown in Table 6.3.

Table 6.3: Chemical composition of H-ZSM-12 zeolite exchanged with ammonium fluoride impregnated with 2 wt. % of lanthanum.

Sample name	*wt. %*					
	O	Al	Si	La	F	Si/Al
T2	51.82	0.55	38.61	0.00	6.00	70.20
T14	56.59	0.62	36.02	0.63	6.14	58.10

Similar to lanthanum impregnation, cerium impregnation was performed to H-ZSM-12 zeolite exchanged with both ammonium nitrate and ammonium fluoride. As shown in Figure 6.11, crystal patterns were preserved by adding cerium up to 2 wt. %. It was observed that the crystallinity was reduced and the intensity of the main peak was reduced from 527 to 266 a.u when H-ZSM-12 zeolite was impregnated with 0.5 wt. %. The crystallinity was

reduced to 55.38%. This intensity was then increased again to 504 a.u. at 1.0 wt. % cerium impregnation and the crystallinity was 98.14. Then the crystallinity was reduced again and the intensity of the main peaks reached to 192 a.u. when H-ZSM-12 zeolite was impregnated with 2 wt. % of cerium where the crystallinity was 41.57%.

H-ZSM-12 zeolite exchanged with ammonium fluoride was also impregnated with 2 wt. % of cerium. As shown in Figure 6.12, the XRD pattern was preserved and the intensity of impregnated sample was reduced from 682 to 471 a.u. where the crystallinity was reduced to 72.22%. Comparing with lanthanum impregnation, cerium has a higher crystallinity than lanthanum at 2 wt. % loading where the crystallinity was 72.22% in the presence of cerium and 68.30% in the presence of lanthanum. Also zeolite exchanged with ammonium fluoride and impregnated with 2 wt. % of cerium has higher crystallinity compared to the one exchanged with ammonium nitrate.

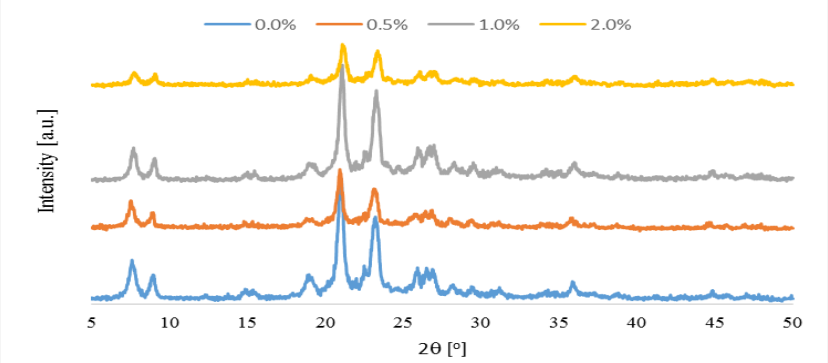

Figure 6.11: XRD patterns of ZSM-12 zeolite exchanged with ammonium nitrate prior to and after cerium impregnation with different load.

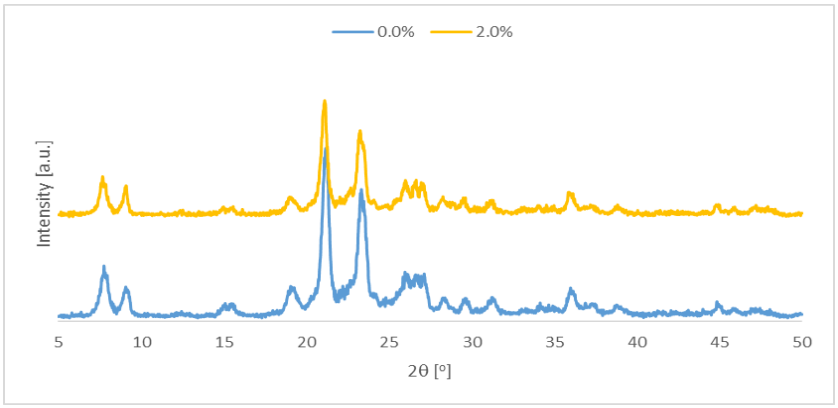

Figure 6.12: XRD patterns of ZSM-12 zeolite exchanged with ammonium fluoride prior to and after cerium impregnation.

Using FE-SEM, crystal size and the morphology of the parent H-ZSM-12 and the treated samples with cerium was observed. As mentioned earlier, the average crystal size of the parent and impregnated samples were 800 nm as shown in Figure 6.13 and 6.14.

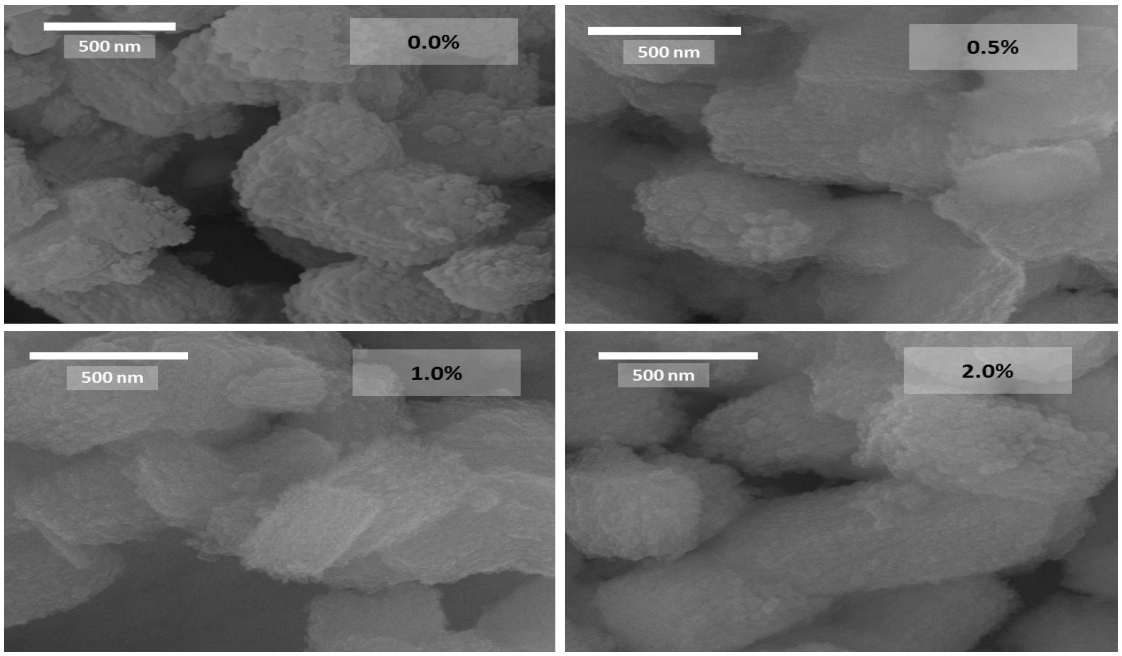

Figure 6.13: FE-SEM micrographs of impregnated ZSM-12 zeolite exchanged with ammonium nitrate prior to and after cerium impregnation with different load.

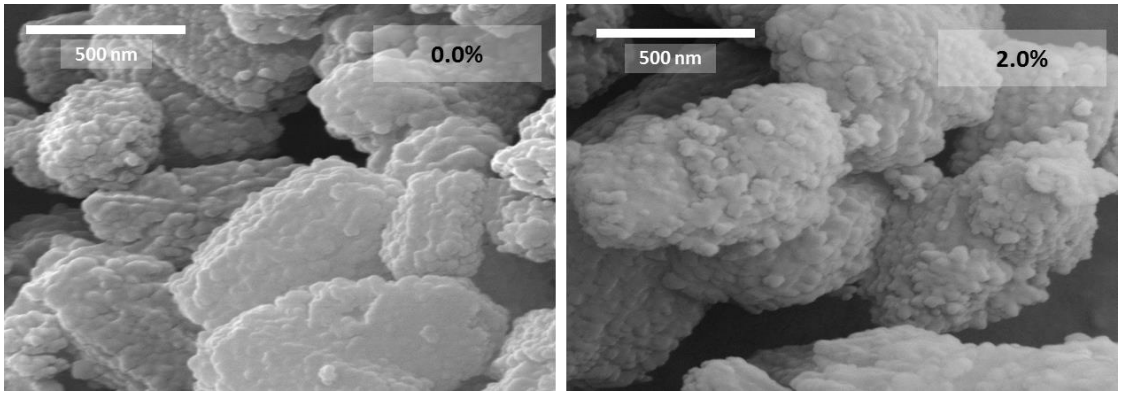

Figure 6.14: FE-SEM micrographs of impregnated ZSM-12 zeolite exchanged with ammonium fluoride prior to and after cerium impregnation with 2.0 wt. %.

Chemical compositions were evaluated using EDX and the presence of cerium was confirmed as shown in Table 6.4. Chemical composition of the samples which impregnated with different concentration of cerium were found to be 0.05, 0.25 and 0.82 wt. %, respectively.

Table 6.4: Chemical composition of H-ZSM-12 zeolite exchanged with ammonium nitrate impregnated with different load of cerium.

Sample name	*wt. %*				
	O	Al	Si	Ce	Si/Al
T1	68.42	0.86	30.72	0.00	35.72
T24	60.97	0.53	34.10	0.05	64.95
T25	69.16	0.58	30.01	0.25	51.74
T26	67.70	0.44	31.04	0.82	70.53

Chemical composition for H-ZSM-12 zeolite exchanged with ammonium fluoride and impregnated with 2 wt. % cerium was also determined with EDX. It was found that the wt. % of fluorine in the tested sample was 28.97 wt. % as shown in Table 6.5. The actual value for fluorine is less than what was observed in the EDX. This is because the chemical composition using EDX is coming from a very small specimen such as 200 nm x 200 nm. Inductively Coupled Plasma (ICP) as an example, provides a more accurate analysis

because large quantity of the samples (e.g. 0.1 mg) can be analyzed and the results are more uniform than EDX.

Table 6.5: Chemical composition of H-ZSM-12 zeolite exchanged with ammonium fluoride impregnated with 2 wt. % of cerium.

Sample name	*wt. %*					
	O	Al	Si	Ce	F	Si/Al
T2	51.82	0.55	38.61	0.00	6.00	70.20
T32	40.09	0.76	29.64	0.53	28.97	39.00

Similar to lanthanum and cerium impregnation, H-ZSM-12 zeolites exchanged with both ammonium nitrate and ammonium fluoride were impregnated with boron. As shown in Figure 6.15, crystal patterns were preserved in the range of 0 and 2 wt. % of boron impregnation. It was observed that the crystallinity was reduced and the intensity of the main peak was reduced from 527 to 387 a.u when H-ZSM-12 zeolite was impregnated with 0.5 wt. %. And the crystallinity was reduced to 78.96 %. As the impregnation load was increased to 1.0 wt. %, the crystallinity was further decreased to 78.46% and the main peak height dropped to 356. Then a sudden increase in the crystallinity to 135.12% and the intensity of the main peak jumped to 765 a.u.

H-ZSM-12 zeolite exchanged with ammonium fluoride was also impregnated with 2 wt. % of boron. As shown in Figure 6.16, the XRD pattern was preserved and the intensity of impregnated sample was reduced from 682 to 506 a.u. and the crystallinity was reduced to 77.81%. Comparing with lanthanum and cerium impregnation, boron has a higher crystallinity than both lanthanum and cerium at 2 wt. % loading. When the zeolite

exchanges with ammonium fluoride and impregnated with 2 wt. % boron, the crystallinity is lower than the one exchanged with ammonium nitrate.

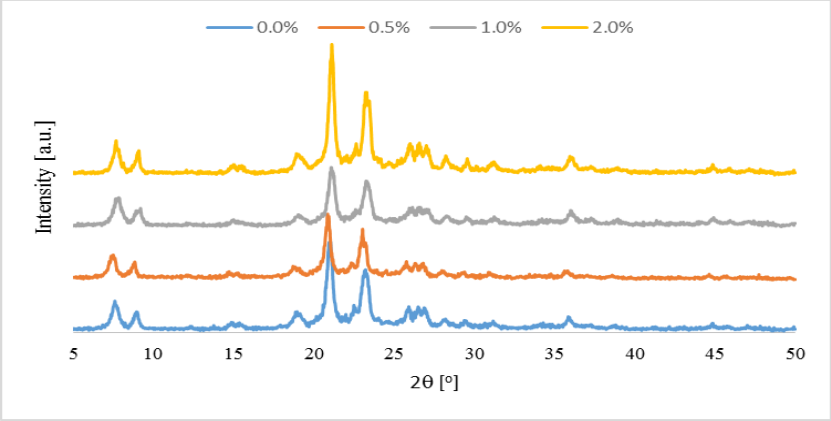

Figure 6.15: XRD patterns of ZSM-12 zeolite exchanged with ammonium nitrate prior to and after boron impregnation with different load.

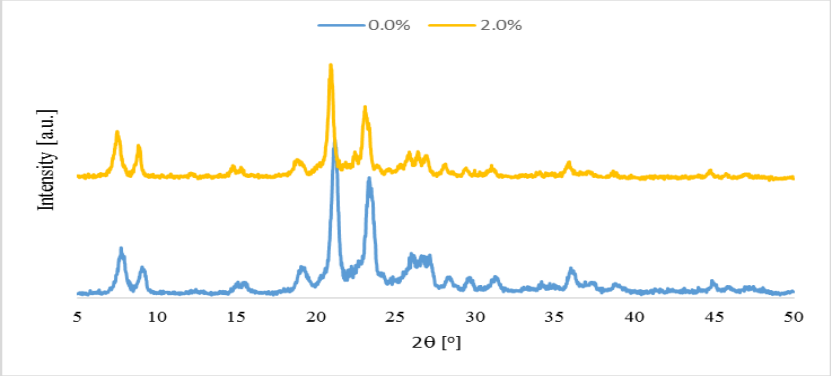

Figure 6.16: XRD patterns of ZSM-12 zeolite exchanged with ammonium fluoride prior to and after boron impregnation.

FE-SEM was used to identify both crystal size and the morphology of the parent H-ZSM-12 and the treated samples with boron. It was observed that the average crystal size of the parent and impregnated samples were 800 nm as shown in Figure 6.17 and 6.18 in the absence and presence of fluorine ions .

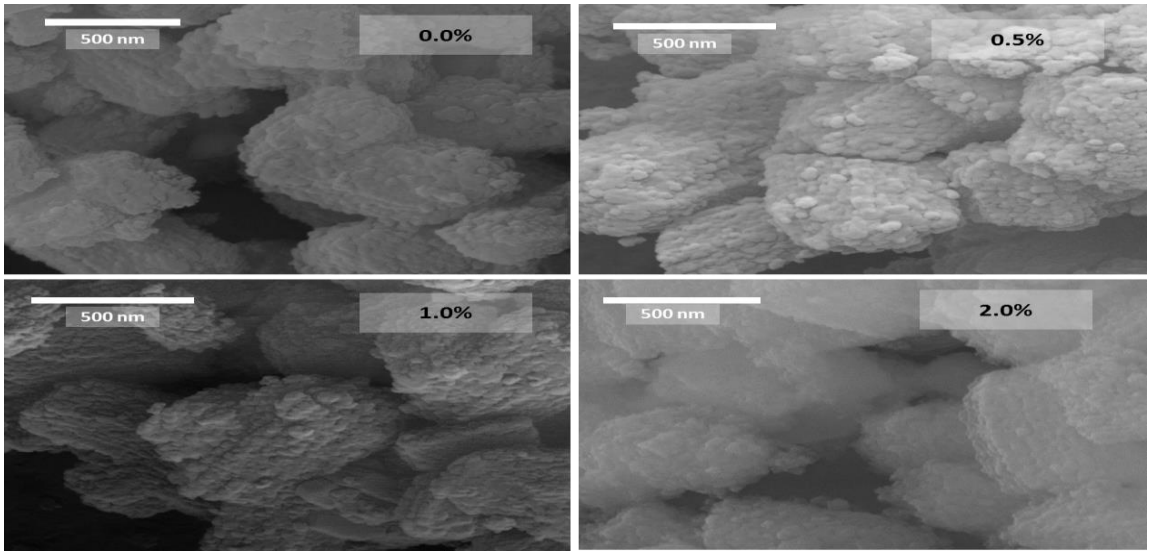

Figure 6.17: FE-SEM micrographs of impregnated ZSM-12 zeolite exchanged with ammonium nitrate prior to and after boron impregnation with different load.

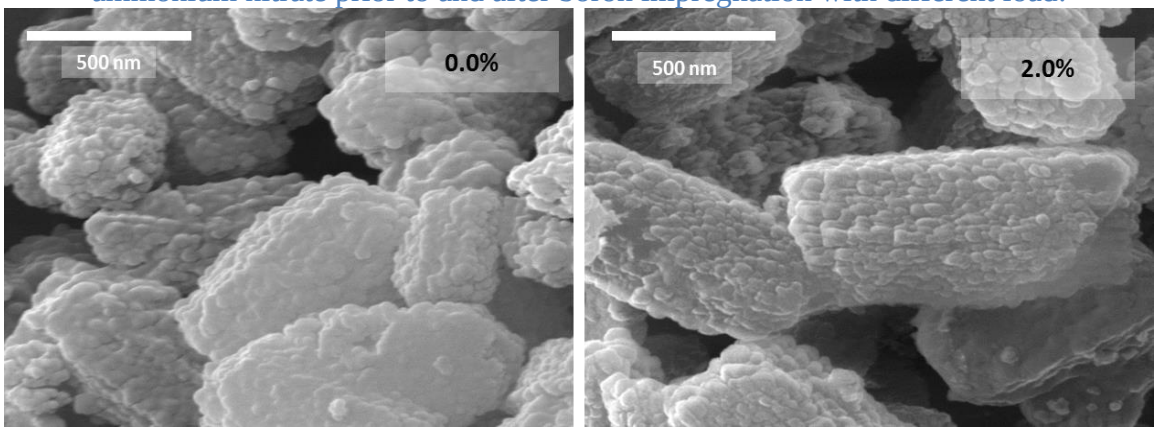

Figure 6.18: FE-SEM micrographs of impregnated ZSM-12 zeolite exchanged with ammonium fluoride prior to and after boron impregnation with 2.0 wt. %.

Using EDX, chemical compositions were evaluated and the presence of boron was confirmed as shown in Table 6.6. Chemical composition of the samples which impregnated with different concentration of boron were found to be 4.81, 7.51 and 5.60 wt. %, respectively. As we observed, the concentration of boron was more than what we impregnated and this means less uniform distribution of boron on the zeolite surface. The impregnation was high in one part of the specimen and low on the other. This can be explained by the difficulty of boric acid dissolving in ethanol and water.

Table 6.6: Chemical composition of H-ZSM-12 zeolite exchanged with ammonium nitrate impregnated with different load of boron.

Sample name	*wt. %*				
	O	Al	Si	B	Si/Al
T1	68.42	0.86	30.72	0.00	35.72
T33	60.63	0.70	33.38	4.81	47.69
T34	92.31	0.82	44.47	7.51	54.23
T35	62.88	0.32	31.19	5.60	97.47

Chemical composition for H-ZSM-12 zeolite exchanged with ammonium fluoride and impregnated with 2 wt. % boron was also determined with EDX. It was found that the wt. % of fluorine in the tested sample was 3.57 wt. % as shown in Table 6.7.

Table 6.7: Chemical composition of H-ZSM-12 zeolite exchanged with ammonium fluoride impregnated with 2 wt. % of boron.

Sample name	*wt. %*					
	O	Al	Si	B	F	Si/Al
T2	51.82	0.55	38.61	0.00	6.00	70.20
T41	56.82	0.40	26.10	12.50	3.57	65.25

CHAPTER 7

CRACKING OF N-HEXANE OVER ZSM-12 ZEOLITE

7.1. Introduction

Many chemical reactions are required to be improved in order to enhance the reaction rate toward the desired products. These reactions are mostly accomplished over heterogeneous catalysts to enhance the conversion. In refinery and petrochemical industries, zeolites are one of the most important heterogeneous catalysts due its importance in shape selectivity. Zeolites properties can highly affect the selectivity towards either the desired or undesired products. Extensive studies are essential to produce zeolites carrying different kind of characteristic based on the demand of a particular reaction. Most of the physical property of zeolites particularly both Lewis and Brønsted acid sites, textural properties such as surface area and pore volume, and zeolite stability is highly affected by the kind and nature of the zeolite [79, 110]. In all cases, zeolite modifications can enhance the catalytic properties for many kinds of reactions such as alkylation, isomerization and cracking based on the nature of the modified zeolites.

Zeolites can be modified by many approaches such as adding silane group, adding fluoride media to establish the hydrophobicity, introducing the mesoporosity and adding additional

materials which may act as an additional catalyst [30, 87, 90, 111]. Adding additional materials to the zeolite frameworks such as metals and semi metals can be performed by several techniques such as impregnation or ion-exchange to obtain co-catalysts material [13, 99, 102].

Zeolites are available with different topology such as MFI, TON and MTW zeolites [14]. Each zeolite has a special building unit, channel system and the number of member ring which allow the zeolite to be hired for a particular reaction rather than another.

In this chapter, we will test the modified MTW zeolite with lanthanum in the catalytic cracking of n-hexane.

7.2. Results and discussion

As a model reaction for the modified MTW zeolite, n-hexane was cracked in a fixed bed reactor 10 mm ID. The reactor tube is made from haste alloy. Different zeolites were evaluated at 650 ^{o}C and atmospheric pressure. These samples named T1, T8, T26 and T35. Where T1 is a parent sample in the form of H-ZSM-12 zeolite exchanged with ammonium nitrate. T8 was obtained by impregnating T1 with 2 wt. % of lanthanum ions. T26 is the modified sample of T1 by impregnating the sample with 2 wt. % of cerium. Similarly, T35 is the modification of T1 by adding 2 wt. % of boron.

Catalytic cracking of n-hexane was performed and the product was evaluated using gas chromatography packed with flammable ionization detector (FID) and thermal conductor detector (TCD). The conversion of n-hexane was calculated using equation 7.1. However, the selectivity was evaluated using equation 7.2.

Equation 7.1: Conversion equation:

$$Conversion\ \% = \left(1 - \frac{n_{n-hexane_{final}}}{n_{n-hexane_{initial}}}\right) x100$$

Where:

$$n_{n-hexane_{final}} = unreacted\ n-hexane$$

$$n_{n-hexane_{initial}} = fed\ n-hexane$$

Equation 7.2: Selectivity equation:

$$Selectivity\ (\ wt.\%) = \frac{w_i}{w_{total}} x100$$

Where

$$w_i = weight\ of\ each\ product$$

$$w_{total} = Total\ weight\ of\ products$$

In the parent (T1), the reaction was carried out for 240 min. It was observed that the conversion of n-hexane was 85.4% after 1 h. This conversion was reduced in a

stepwise manner until it reached to 60% after 240 min as shown in Figure 7.1. During the whole reaction time, the average conversion was 68.8%. The total deactivation generally was calculated from the difference between the conversion of the first and last time. It was found that the deactivation is 25.4 for T1. The minimum and maximum selectivity toward the olefin was 54.3% and 76%, respectively, as shown in Figure 7.1. The average selectivity to olefin through the time on stream was 68.3%. Among the olefin, the average selectivity toward both propylene and ethylene were the maximum and their selectivity represent 54.1% of all olefin and the average of propylene to ethylene ratio was 1.7. The olefin composition was calculated and shown in Figure 7.2.

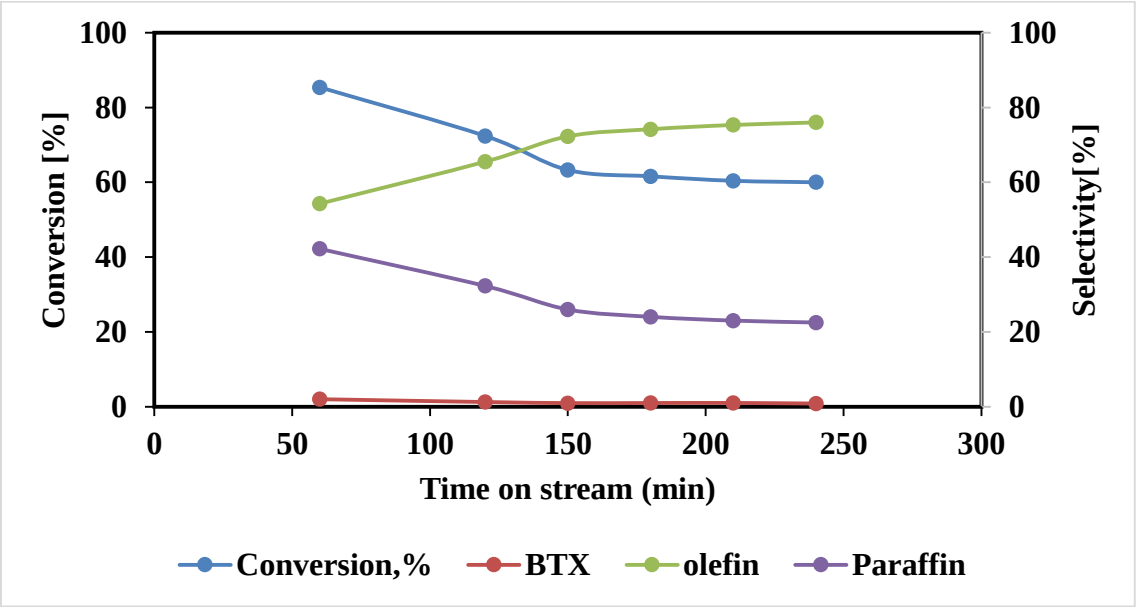

Figure 7.1: Conversion and selectivity of n-hexane cracking over T1.

`

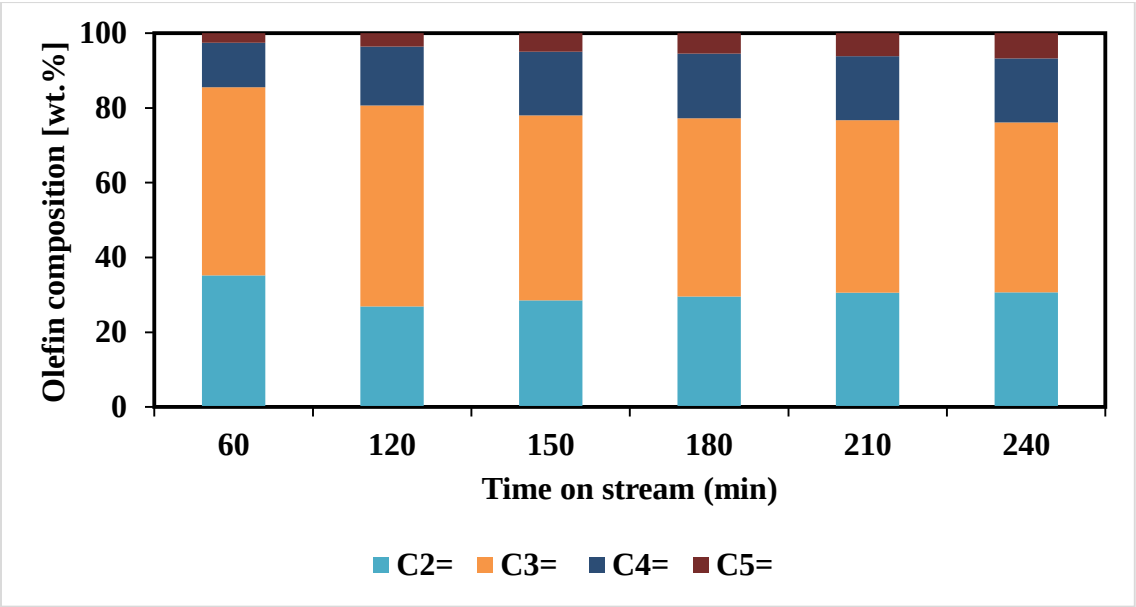

Figure 7.2: Olefin composition of n-hexane cracking over T1.

In the modified sample with 2 wt. % of lanthanum (T8), cracking of n-hexane was carried out at 650 ^{o}C with reaction time of 240 min. The conversion of n-hexane was 79.5% after 1 h of reaction. This conversion was decreased with time until it reached 57.1% after 240 min as shown in Figure 7.3. The average conversion was 63.6%. As compared to the parent zeolite (T1), the conversion is smaller insignificantly. However, by calculating the difference of conversion, there is a small improvement in the deactivation compared to T1.

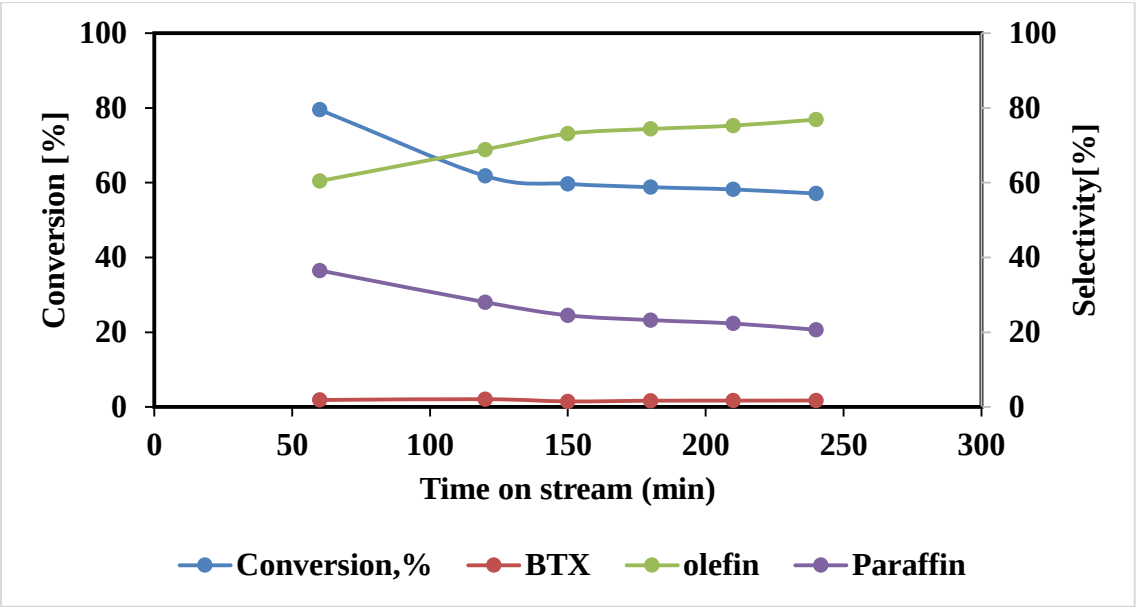

Figure 7.3: Conversion and selectivity of n-hexane cracking over T8.

The minimum and maximum selectivity toward the olefin was 60.5% and 76.9%, respectively, as shown in Figure 7.3. The average selectivity to olefin through the time on stream was 70.4%. Among the olefin, the average selectivity toward both propylene and ethylene were the maximum and their selectivity represent 56.6% of all olefin. It was observed that there was an improvement in the selectivity toward both propylene and ethylene compared to T1. However, a small reduction in the average of propylene to ethylene ratio (P/E). In T8, P/E was 1.5. The olefin composition was shown in Figure 7.4.

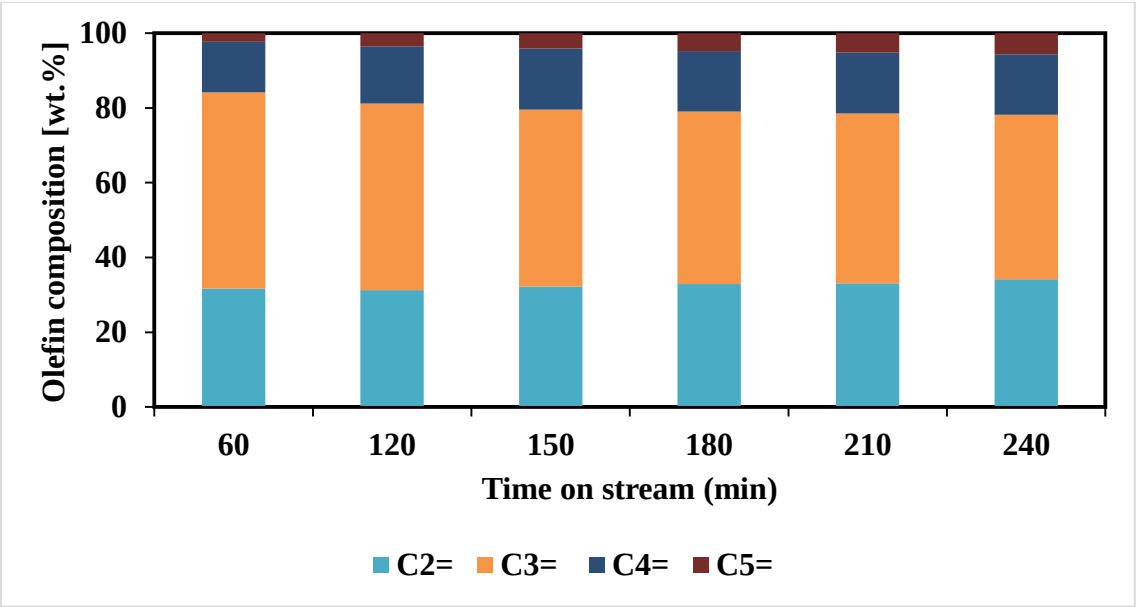

Figure 7.4: Olefin composition of n-hexane cracking over T8.

Cerium was also used to modify the parent sample. Zeolite impregnated with 2 wt. % of cerium (T26) was prepared and its performance was tested in the cracking of n-hexane and compared to both parent and lanthanum modified zeolite. The reaction was carried out at 650 ^{o}C with reaction time of 240 min. It was observed that the conversion was 73.4% after 1 h of reaction. This conversion was decreased with time until it reached 56.2% after 240 min as shown in Figure 7.5. The average conversion was 63.4%. As compared to both T1 and T8, the conversion was less than both T1 and T8 with total decrease of 5.2% and 0.2%, respectively. However, by calculating the difference of conversion, there is further improvement in the deactivation compared to T1 and T8.

The minimum and maximum selectivity toward the olefin was 63.8% and 77.7%, respectively, as shown in Figure 7.5. The average selectivity to olefin through the

time on stream was 71.3%. Propylene and ethylene were represented most of the olefin with an average selectivity of 56.7% of all olefin. Comparing to both T1 and T8, there was an improvement in the selectivity to olefin particularly both propylene and ethylene. The improvement was +2.6% and +0.2% compared to both T1 and T8, respectively. However, very small reduction in the average of propylene to ethylene ratio (P/E) compared to T1 (-0.1) and small improvement was achieved compared to T8 (+0.1). In T26, P/E was 1.6. The olefin composition was shown in Figure 7.6.

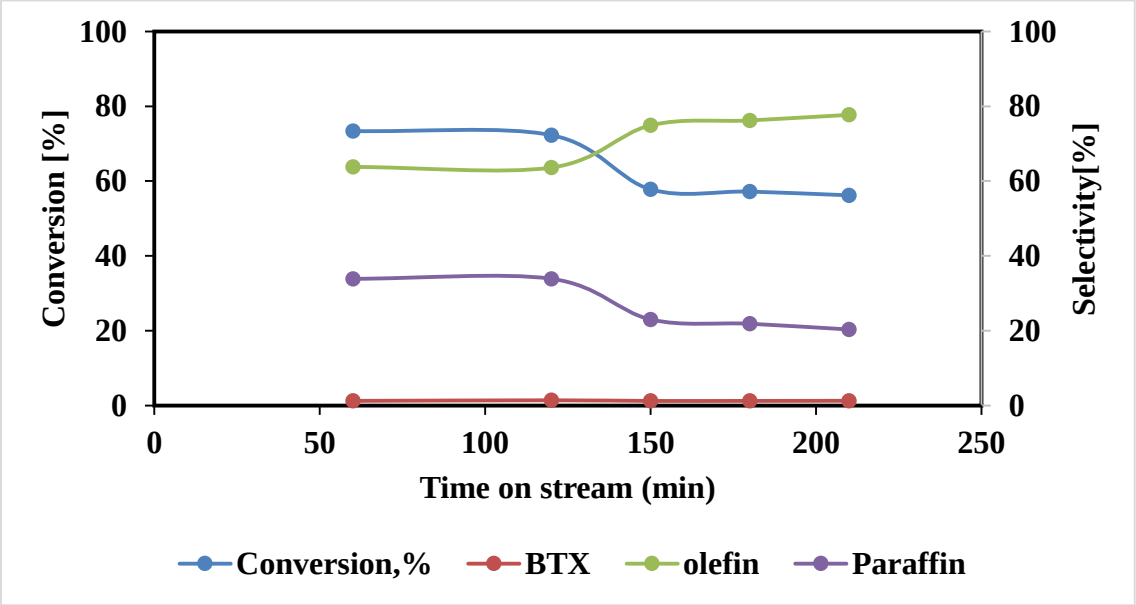

Figure 7.5: Conversion and selectivity of n-hexane cracking over T26.

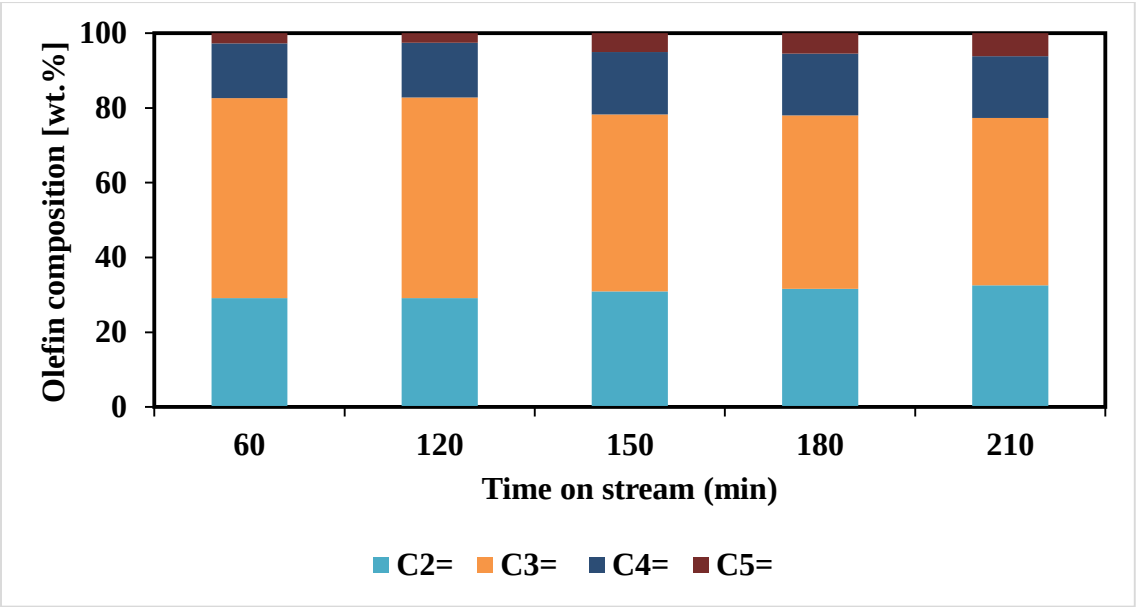

Figure 7.6: Olefin composition of n-hexane cracking over T26.

Semi-metal was also used in the modification of T1. Boron (2 wt. %, T35) was used to modify the parent samples. Its performance was observed in the cracking of n-hexane and compared to the parent, lanthanum and cerium modified zeolites. The reaction was carried out at 650 ^{o}C with reaction time of 240 min. It was observed that the conversion was 76.4% after 1 h of reaction. This conversion was decreased with time until it reached 59 % after 240 min as shown in Figure 7.7. The average conversion was 65.1%. As compared to T1, T8 and T26, the conversion was less than T1 (-3.5) insignificantly and it was better than both T8 and T26 with +1.5% and +1.7% difference, respectively. However, by calculating the difference of conversion, there is further improvement in the deactivation compared to T1, T8 and T26.

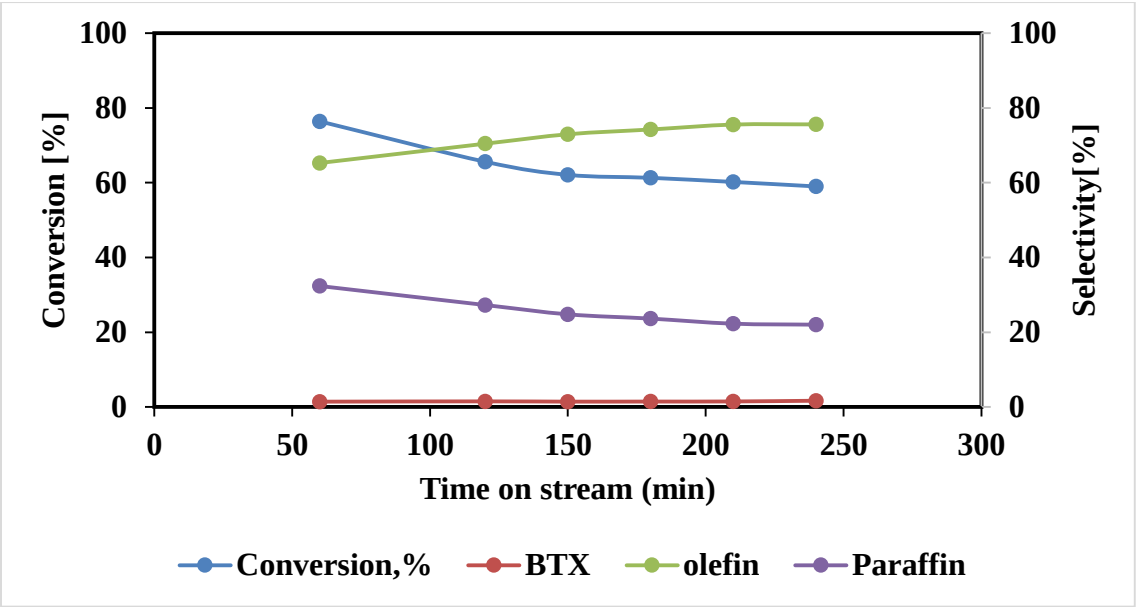

Figure 7.7: Conversion and selectivity of n-hexane cracking over T35.

The minimum and maximum selectivity toward the olefin was 65.3% and 75.6%, respectively, as shown in Figure 7.7. The average selectivity to olefin through the time on stream was 71.7%. Highest quantity of light olefin was both propylene and ethylene which represent 57.4% of selectivity of all olefin. T35, was represented the best improvement in selectivity toward olefin and particularly propylene and ethylene. The improvement of selectivity toward both propylene and ethylene were +3.2%, +0.8% and +0.6% compared to T1, T8 and T26, respectively. However, the ratio of propylene to ethylene ratio (P/E) was same as the parent sample (T1). The olefin composition was shown in Figure 7.8.

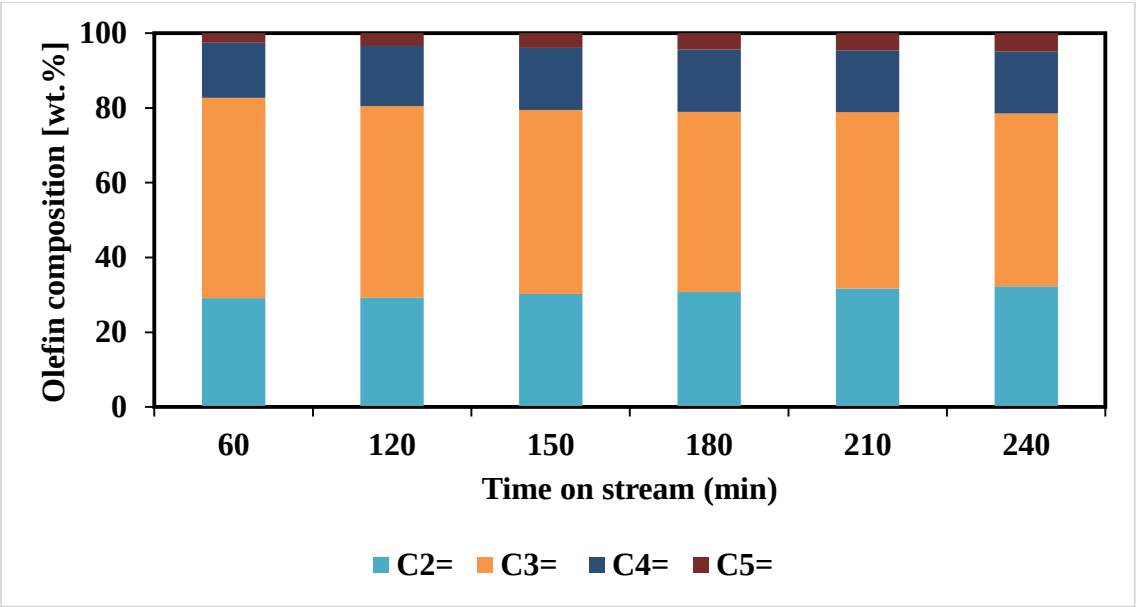

Figure 7.8: Olefin composition of n-hexane cracking over T35.

As shown in Table 7.1, summary of average selectivity in all modified samples. Olefin compositions of n-hexane cracking over modified ZSM-12 zeolite are shown in Table 7.2.

Table 7.1: Average selectivity of n-hexane cracking over modified ZSM-12 zeolite.

Selectivity, %				
Compound names	T1	T8	T26	T35
C3= + C2=	54.1	56.6	56.7	57.4
Propylene	33.7	33.8	34.8	35.7
Ethylene	20.5	22.7	21.9	21.7
BTX	1.2	1.8	1.3	1.5
olefin	68.3	70.4	71.3	71.7
Paraffin	29.5	26.9	26.6	26.1

Table 7.2: Olefin composition of n-hexane cracking over modified ZSM-12 zeolite.

Olefin composition				
Compound names	T1	T8	T26	T35
C2=	30.2	32.2	30.7	30.2
C3=	49.5	48.3	49.1	49.9
C4=	15.8	15.5	15.8	16.1
C5=	4.6	4.0	4.4	3.8

Using different kind of metals and semi-metals can improve the properties of the external and internal surface of the zeolite. In the catalytic cracking of n-hexane, both Lewis and Brønsted are demands to enhance the selectivity and the conversion of the reactant. More Brønsted acid particularly, can enhance the fast and random catalytic cracking of the feed. This can lead to the reduction of the selectivity. Lewis acid, on the other hand, is important for the cracking too. But higher selectivity can be obtained. Tuning these acids can led to higher selectivity. Aluminum in the zeolite framework, can donate the Brønsted acid. However, the reduction of the conversion on the lanthanum and cerium modified MTW zeolite is due to the location of these ions in the framework. Lanthanum and cerium most probably either exchanged by some aluminum ions or located near to the aluminum ions. On the other hand, boron mostly can be connected with the Lewis acid and can contribute to both Lewis and Brønsted. This effect can be noticed from both weak and strong acid sites as shown in Figure 7.9.

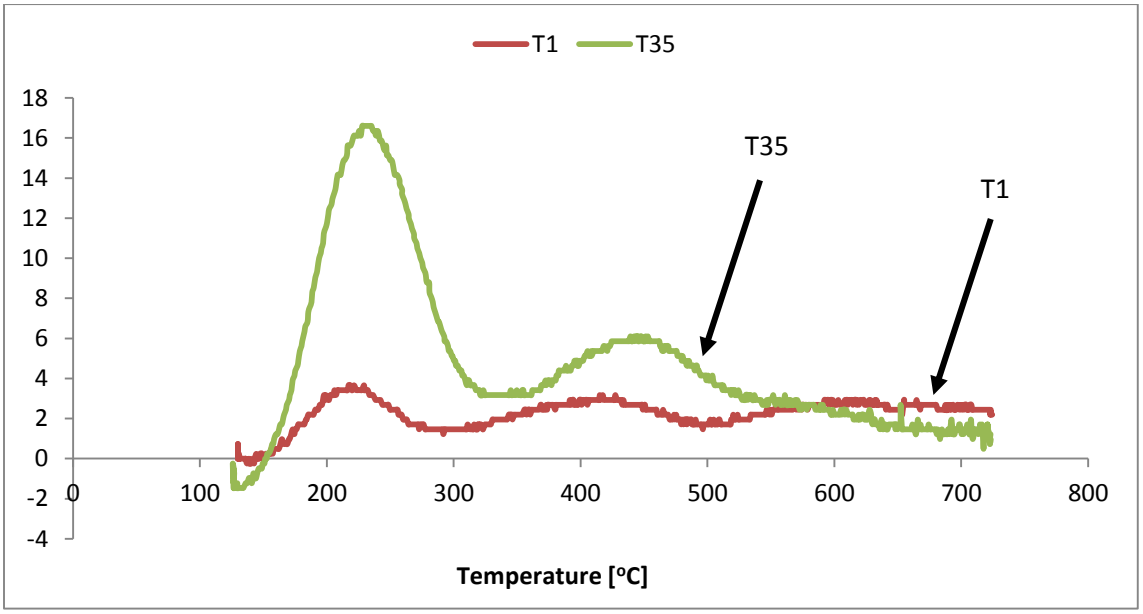

Figure 7.9: Effect of boron in increasing both weak and strong acids.

CHAPTER 8

STABILITY ON HOT WATER

8.1. Introduction

Zeolites can be used in many fields in refinery and petrochemical industries due to their pore structure and high activity. Zeolites composes of both silicon and aluminum. Zeolite has both Lewis and Brønsted acid sites. Aluminum in zeolites can enhance the reactivity due to the presence of acid sites. Reactions in refinery industries requires certain amount of both Brønsted and Lewis acid sites. It was observed that as Si/Al ratio increases, the thermal stability of the zeolite increases [112].

Zeolite stability is one of the most important concern in catalytic reactions [113-115]. In petrochemical industries, zeolites can be interacted with water or steam. Interaction with water or steam can affect both acidity and the crystallinity on the zeolites. Due to this interaction, atoms such as silicon and aluminum can be removed from zeolites frameworks. As a result, extra-framework generates from the removal of some ions [116].

Zeolite stability can be tested with many techniques. One of these techniques is the hydrothermal stability of the zeolite in hot liquid water [114]. Water in this stage, consists

of two parts namely proton and hydroxide ions. Proton ions (H^+) from the water, attack the -Si-O-Al- bonds in the framework to form Al and HO-Si as extra-framework [113]. However, the hydroxide ions attack the –Si-O-Si- to form 2 Si-OH as extra-framework [113]. Removal of silicon ions is called desilication and removal of aluminum is dealumination. These processes is highly affect the acidity of the zeolites and the phase crystallinity.

In this chapter, the hydrothermal stability of modified ZSM-12 zeolites impregnated with lanthanum, cerium and boron were estimated in the presence of hot liquid water. Effect of lanthanum, cerium and boron were studied and compared with the parent zeolite.

8.2. Results and discussion

Samples were heated in hot liquid water for 72 h at 200 ^oC. In 30 g of deionized water, 0.2 g of H-ZSM-12 zeolite was added. After 72 h, samples were quenched in water to allow the fast cooling. The samples were dried and characterized by XRD. In the parent zeolite, it was observed that the crystallinity was preserved and the intensity of the main peak was reduced insignificantly from 527 to 519 a.u. as shown in the XRD patterns in Figure 8.1. The crystallinity was reduced to 96.5 % after 72 h.

Using NH_3-TPD, the weak and strong acid sites were determined. Comparing the TPD before and after hot liquid water treatment (T1 and T1-72h), we observed there is increase

in both weak and strong acid sites. This means there was both desilication and dealumination were happened. NH_3-TPD of T1 before and after hot liquid water treatment is shown in Figure 8.2.

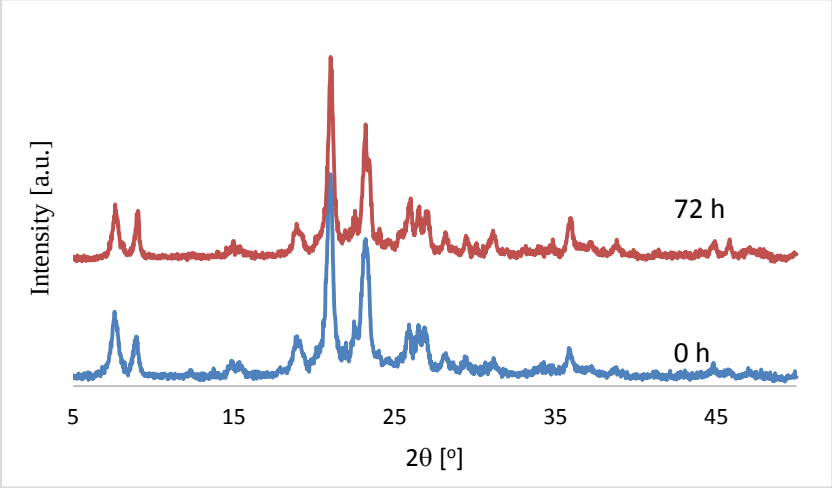

Figure 8.1: XRD patterns before and after hydrothermal treatment of T1.

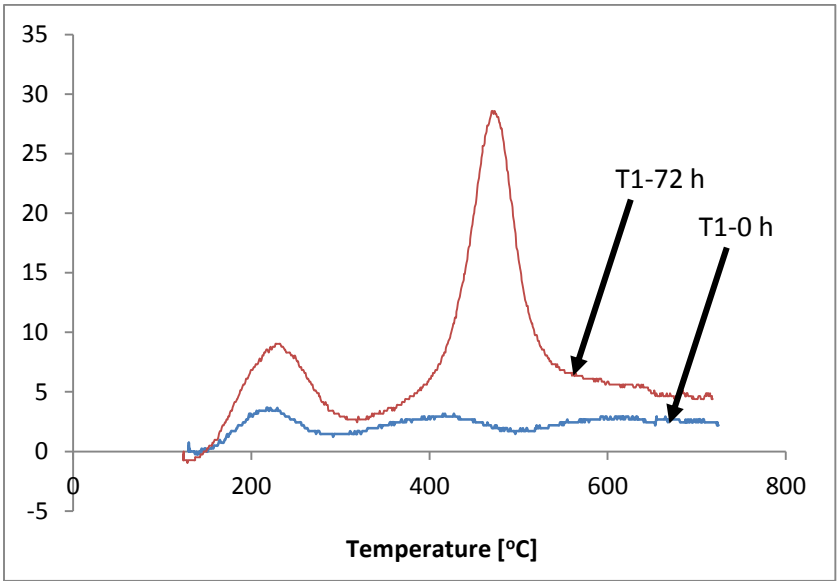

Figure 8.2: NH3-TPD for T1 before and after hot liquid water treatment.

The stability of ZSM-12 zeolite modified in the presence of lanthanum was also tested in hot liquid water. It was observed a reduction in the intensity of the main peak from 361 to 225 a.u. as shown in Figure 8.3. The crystallinity was reduced to 66.70%.

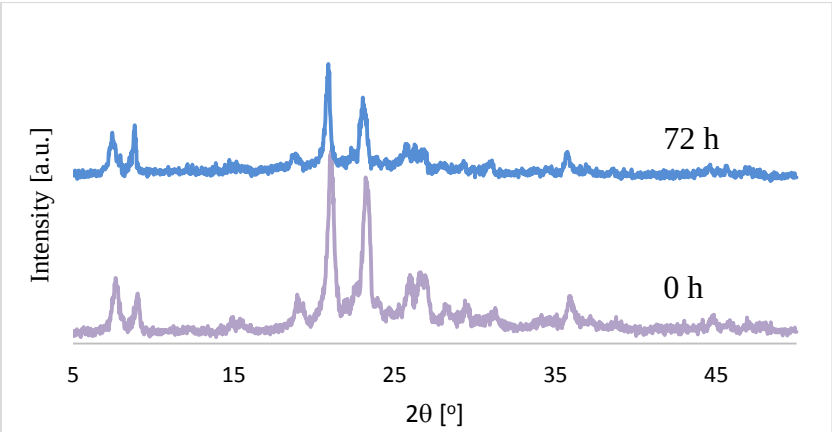

Figure 8.3: XRD patterns before and after hydrothermal treatment of T8.

In the presence of boron, we observed that the intensity of the main peak decreased from 765 a.u. to 397 as shown in Figure 8.4. The crystallinity was reduced to 59.34. In all cases, small crystallinity can be lost by adding the metals or semi-metals only if we can gain other features such as conversion and selectivity toward the desired products. Here, in the presence of boron, there is a small reduction in the crystallinity but there is an improvement in both conversion and selectivity to olefin.

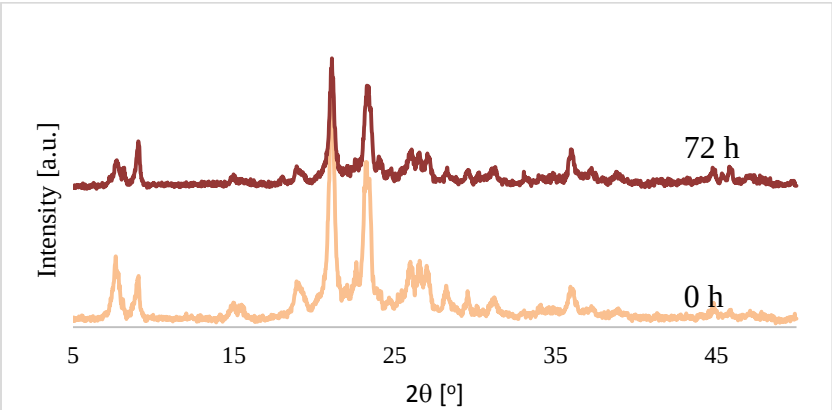

Figure 8.4: XRD patterns before and after hydrothermal treatment of T35.

Using NH_3-TPD, the weak and strong acid sites were determined. In T35, the weak acid site was more than after treatment with hot water for 72 h. However, the strong acid was small. In T35 after 72 h treatment, the weak acid site was negligible and the strong acid site

was very large compared with the untreated sample as shown in Figure 8.5. The decrease in the weak acid site and increase in the strong acid site is an evidence for the desilication process.

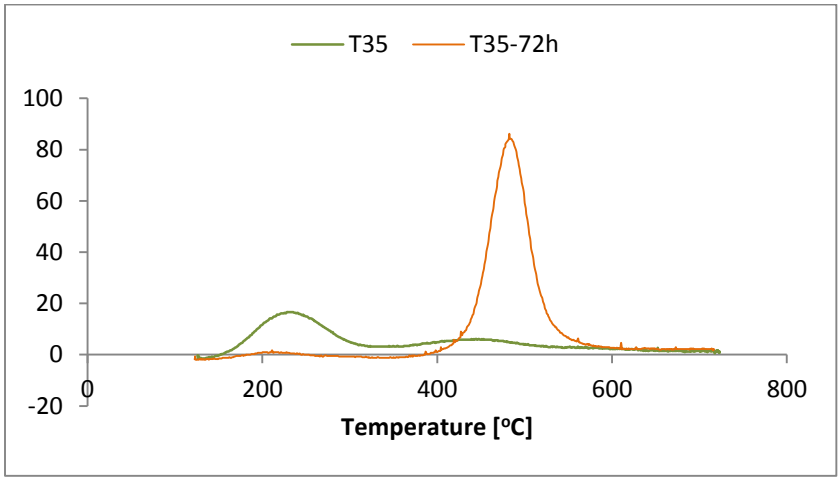

Figure 8.5: NH3-TPD for T35 before and after hot liquid water treatment.

By integrating the area under each peak, the quantity of weak acid and strong acid were determined as shown in Table 8.1.

Table 8.1: Acid strength before and after hot water treatment.

	Acid strength (mmol/g)			
Sample	Weak 181.1-253.4	Strong 384.6-599.2	Total acidity	Weak/Strong
T1	0.213	0.712	0.925	0.300
T1-72	0.541	2.652	3.193	0.204
T35	0.986	0.902	1.889	1.093
T35-72	0.041	5.055	5.095	0.008

CHAPTER 9

CONCLUSION AND RECOMMENDATIONS

9.1. Conclusion

Pure ZSM-12 zeolite can be synthesized in large range of SiO_2/Al_2O_3 between 160 and 400. In order to obtain pure ZSM-12 zeolite, alkalinity need to be adjusted beside the synthesis temperature and synthesis time. Alkalinity ratio $NaOH/SiO_2$ can be varied between 0.132 and 0.156. We succeeded to obtain pure ZSM-12 zeolite with different silica to alumina ratio, particularly ratios of 160, 280 and 400. Evaluating the catalytic performance was performed using n-hexane. The target of our research is to obtain higher selectivity to olefin. We tried to find the optimum silica to alumina ratio, which give us the best selectivity to olefin especially propylene and ethylene and we found that the optimum silica to alumina is 160. Then we fixed our modification to be at this silica to alumina ratio and we tried to modify ZSM-12 by desilication and impregnation. In desilication, the modification was performed only as a pre-introduction to see the improvement in pore volume, surface area and acid sites which can be further modified by impregnation. We found that the microwave irradiation offered shorter treatment time in the presence of alkaline solution such as sodium hydroxide than the conventional hydrothermal method. The mesopores were introduced with different level of mesoporosity and the microporosity was decreased by increasing the concentration of the alkaline solution. At 0.1 M for 5 and 10 min of treatment time and at

0.2 M for 5 min both mesopore and micropore were obtained and the obtained materials can be called a hierarchical zeolite. Longer than this time and higher concentration led to the loss of micropores. The specific surface area was increased. After certain concentration and treatment time, it started to increase incrementally but not up to the parent zeolite. Parent zeolite was impregnated with lanthanum, cerium and boron. In the presence of lanthanum, the selectivity to olefin was 70.4%, which is better than the parent by +2.1%. However, in the presence of cerium, the selectivity to olefin was better than the parent by +2.9%. Boron was the best in the selectivity to olefin compared to the parent by improvement of +3.4%. However, the conversion was in the following order T1> T35> T8> T26 by a difference of 5.0% between T1 and T26. The stability on hot liquid water was performed at 200 ^{o}C for 72 h. It was observed that the crystallinity in the parent zeolite was reduced to 96.5%. However, in the presence of lanthanum and boron, crystallinity was reduced to 66.70 and 59.34 %, respectively. NH_3-TPD was shown both desilication and dealumination in the parent. In the presence of boron, the strong acid was too intense and desilication was observed.

9.2. Recommendations

From the results of our experiments we can recommend the following items to be done for further modifications:

1. Desilication of ZSM-12 zeolite followed by dealumination
2. Impregnation the desilicated sample
3. Impregnation the desilicated and dealuminated sample
4. Study the effect of co-impregnation and tri-impregnation

APPENDICES

APPENDIX A

Zeolite synthesis

The values of X, Y and Z of ZSM-12 zeolite synthesis are shown in Table A.1.

Table A.1: The weight of synthesized samples.

Name	SiO_2/Al_2O_3	X (g, NaOH)	Y (g, H_2O)	Z (g, $Al_2(SO_4)_3$ 18 H_2O)
S1	160	1.07	14.05	0.79
S2	160	1.09	14.05	0.79
S3	160	1.14	14.06	0.79
S4	160	1.18	14.05	0.79
S5	240	1.09	14.18	0.53
S6	280	1.14	14.22	0.45
S7	320	1.00	14.24	0.39
S8	320	1.04	14.24	0.39
S9	320	1.09	14.24	0.39
S10	320	1.14	14.24	0.39
S11	320	1.18	14.24	0.39
S12	360	1.09	14.24	0.35
S13	400	1.09	14.28	0.32

The molar ratios of the synthesized zeolite samples are shown in Table A.2.

Table A.2: Molar ratio of synthesized samples.

Name	Molar ratio of the gel mixture
S1	**1 SiO_2:0.1235 TEABr: 0.0063 Al_2O_3: 0.0705 Na_2O: 12.57 H_2O**
S2	**1 SiO_2:0.1235 TEABr: 0.0063 Al_2O_3: 0.072 Na_2O: 12.57 H_2O**
S3	**1 SiO_2:0.1235 TEABr: 0.0063 Al_2O_3: 0.0750 Na_2O: 12.57 H_2O**
S4	**1 SiO_2:0.1235 TEABr: 0.0063 Al_2O_3: 0.0778 Na_2O: 12.57 H_2O**
S5	**1 SiO_2:0.1235 TEABr: 0.0042 Al_2O_3: 0.0720 Na_2O: 12.57 H_2O**
S6	**1 SiO_2:0.1235 TEABr: 0.0036 Al_2O_3: 0.0720 Na_2O: 12.57 H_2O**
S7	**1 SiO_2:0.1235 TEABr: 0.0031 Al_2O_3: 0.0660 Na_2O: 12.57 H_2O**
S8	**1 SiO_2:0.1235 TEABr: 0.0031 Al_2O_3: 0.0686 Na_2O: 12.57 H_2O**

S9	**1 SiO_2:0.1235 TEABr: 0.0031 Al_2O_3: 0.0719 Na_2O: 12.57 H_2O**
S10	**1 SiO_2:0.1235 TEABr: 0.0031 Al_2O_3: 0.0752 Na_2O: 12.57 H_2O**
S11	**1 SiO_2:0.1235 TEABr: 0.0031 Al_2O_3: 0.0778 Na_2O: 12.57 H_2O**
S12	**1 SiO_2:0.1235 TEABr: 0.0028 Al_2O_3: 0.0719 Na_2O: 12.57 H_2O**
S13	**1 SiO_2:0.1235 TEABr: 0.0025 Al_2O_3: 0.0720 Na_2O: 12.57 H_2O**

APPENDIX B

Weak and strong acids determination

Weak and strong acid sites were determined using the integration of the curve. Estimating the area under the peak for both strong and weak acid sites. In our analysis, we used Origin software. Both X and Y were filled in the program. Then using the command integrate, the log directly calculate the area as shown in Figure B.1.

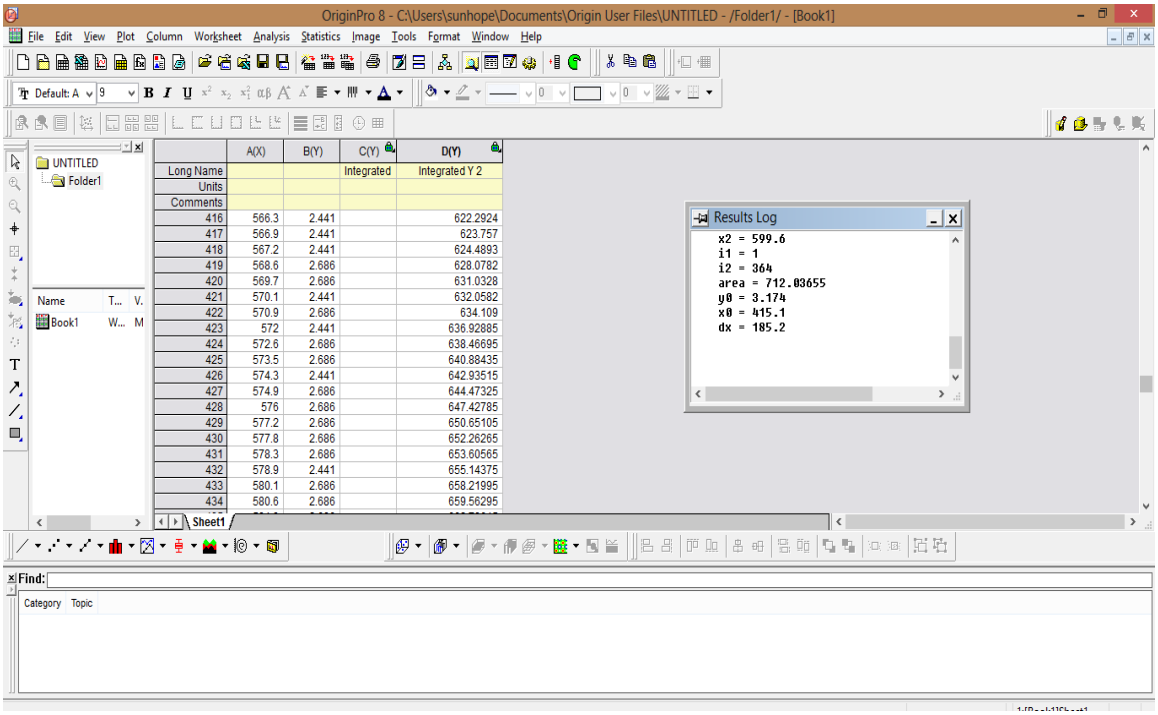

Figure B.1: Origin software for evaluating the area under the peaks

Nomenclature

C	Constant
$n_{n-hexane_{initial}}$	Fed n-hexane (mole)
$n_{n-hexane_{final}}$	Unreacted n-hexane (mole)
P	Equilibrium pressure (kPa)
P_o	Saturation pressure (kPa)
V	Adsorbed gas (ml)
V_m	Monolayer adsorbed gas (ml)
w_i	Weight of each product (g)
w_{total}	Total weight of products (g)
λ	Wavelength (A^o)
$\beta_{1/2}$	Full width half maximum (^{o})
θ	Angle (^{o})

References

1. Maier, C. and T. Calafut, *Polypropylene: The Definitive User's Guide and Databook*. 2008: Elsevier Science.
2. Abeles, F.B., P.W. Morgan, and M.E. Saltveit, *Ethylene in Plant Biology*. 2012: Elsevier Science.
3. Mackay, D., W.Y. Shiu, and K.C. Ma, *Illustrated Handbook of Physical-Chemical Properties and Environmental Fate for Organic Chemicals*. 1993: Taylor & Francis.
4. Bhatia, S., *Zeolite Catalysts: Principles and Applications*. 1989: Taylor & Francis.
5. Yang, R.T., *Adsorbents: Fundamentals and Applications*. 2003: Wiley.
6. Scott M. Auerbach, K.A.C., Prabir K. Dutta, *Handbook of Zeolite Science and Technology*. 2003.
7. Yao, J., et al., *Influence of glycerol cosolvent on the synthesis of size controllable zeolite A.* Materials Letters, 2011. **65**(14): p. 2304-2306.
8. Junaidi, M.U.M., et al., *The effects of solvents on the modification of SAPO-34 zeolite using 3-aminopropyl trimethoxy silane for the preparation of asymmetric polysulfone mixed matrix membrane in the application of CO2 separation.* Microporous and Mesoporous Materials, 2013(0).
9. Xu, F., et al., *Rapid tuning of ZSM-5 crystal size by using polyethylene glycol or colloidal silicalite-1 seed.* Microporous and Mesoporous Materials, 2012.
10. Shang, Y., et al., *Modification of MCM-22 zeolites with silylation agents: Acid properties and catalytic performance for the skeletal isomerization of n-butene.* Catalysis Communications, 2008. **9**(5): p. 907-912.
11. Zanardi, S., et al., *Incorporation of germanium and boron in zeolite chabazite.* Microporous and Mesoporous Materials, 2013. **168**(0): p. 164-170.
12. Garcia Vargas, N., S. Stevenson, and D.F. Shantz, *Simultaneous isomorphous incorporation of boron and germanium in MFI zeolites.* Microporous and Mesoporous Materials, 2013. **170**(0): p. 131-140.
13. Dalla Costa, B.O., M.A. Peralta, and C.A. Querini, *Gas phase dehydration of glycerol over, lanthanum-modified beta-zeolite.* Applied Catalysis A: General, 2014. **472**(0): p. 53-63.
14. Baerlocher, C., L.B. McCusker, and D.H. Olson, *Atlas of Zeolite Framework Types*. 2007: Elsevier Science.
15. Yoo, K., et al., *TEABr directed synthesis of ZSM-12 and its NMR characterization.* Microporous and Mesoporous Materials, 2003. **60**(1–3): p. 57-68.
16. E.J. Rosinski, M.K.R., US Patent 3,832,449, 1974.
17. Trewella, J.C., et al., *The silicon-29 MAS-n.m.r. spectrum of ZSM—12.* Zeolites, 1985. **5**(3): p. 130-131.
18. Fyfe, C.A., et al., *Correlations between lattice structures of zeolites and their 29Si MAS n.m.r. spectra: zeolites KZ-2, ZSM-12, and Beta.* Zeolites, 1988. **8**(2): p. 132-136.
19. LaPierre, R.B., et al., *The framework topology of ZSM-12: A high-silica zeolite.* Zeolites, 1985. **5**(6): p. 346-348.

20. Karge, H.G., P. Anderson, and J. Weitkamp, *Post-Synthesis Modification I*. 2002: Springer.
21. Groen, J.C., J.A. Moulijn, and J. Pérez-Ramírez, *Decoupling mesoporosity formation and acidity modification in ZSM-5 zeolites by sequential desilication–dealumination.* Microporous and Mesoporous Materials, 2005. **87**(2): p. 153-161.
22. S. Mitchell, N.L.M., K. Kunze, J. Pérez-Ramírez, Nature Chem., 2012. **4**: p. 825.
23. A. Bonilla, D.B., J. Pérez-Ramírez, J. Catal., 2009. **265**: p. 170.
24. Abelló, S., A. Bonilla, and J. Pérez-Ramírez, *Mesoporous ZSM-5 zeolite catalysts prepared by desilication with organic hydroxides and comparison with NaOH leaching.* Applied Catalysis A: General, 2009. **364**(1–2): p. 191-198.
25. Biemelt, T., et al., *Hierarchical porous zeolite ZSM-58 derived by desilication and desilication re-assembly.* Microporous and Mesoporous Materials, 2014. **187**(0): p. 114-124.
26. Li, J., et al., *Catalytic fast pyrolysis of biomass with mesoporous ZSM-5 zeolites prepared by desilication with NaOH solutions.* Applied Catalysis A: General, 2014. **470**(0): p. 115-122.
27. Schmidt, F., et al., *Improved catalytic performance of hierarchical ZSM-5 synthesized by desilication with surfactants.* Microporous and Mesoporous Materials, 2013. **165**(0): p. 148-157.
28. Muraza, O., et al., *Controlled and rapid growth of MTT zeolite crystals with low-aspect-ratio in a microwave reactor.* Chemical Engineering Journal, 2013. **226**(0): p. 367-376.
29. Yoo, W.C., et al., *Synthesis of mesoporous ZSM-5 zeolites through desilication and re-assembly processes.* Microporous and Mesoporous Materials, 2012. **149**(1): p. 147-157.
30. Qin, Z., et al., *Mesoporous Y zeolite with homogeneous aluminum distribution obtained by sequential desilication–dealumination and its performance in the catalytic cracking of cumene and 1,3,5-triisopropylbenzene.* Journal of Catalysis, 2011. **278**(2): p. 266-275.
31. Matias, P., et al., *Desilication of a TON zeolite with NaOH: Influence on porosity, acidity and catalytic properties.* Applied Catalysis A: General, 2011. **399**(1–2): p. 100-109.
32. Gil, B., et al., *Desilication of ZSM-5 and ZSM-12 zeolites: Impact on textural, acidic and catalytic properties.* Catalysis Today, 2010. **152**(1–4): p. 24-32.
33. Mokrzycki, Ł. and B. Sulikowski, *Desilication of ZSM-12 and MCM-22 type zeolites and their performance in isomerization of α-pinene*, in *Studies in Surface Science and Catalysis*, P.M. Antoine Gédéon and B. Florence, Editors. 2008, Elsevier. p. 1231-1234.
34. Wei, X. and P.G. Smirniotis, *Synthesis and characterization of mesoporous ZSM-12 by using carbon particles.* Microporous and Mesoporous Materials, 2006. **89**(1–3): p. 170-178.
35. Aguado, J. and D.P. Serrano, *Feedstock Recycling of Plastic Wastes*. 1999: Royal Society of Chemistry.
36. Lloyd, L., *Handbook of Industrial Catalysts*. 2011: Springer.
37. Xu, R., et al., *Chemistry of Zeolites and Related Porous Materials: Synthesis and Structure*. 2009: Wiley.

38. Kalvachev, Y., et al., *Seeds-induced fluoride media synthesis of nanosized zeolite Beta crystals.* Microporous and Mesoporous Materials, 2013. **177**(0): p. 127-134.
39. Kim, D.S., et al., *Synthesis of zeolite beta in fluoride media under microwave irradiation.* Microporous and Mesoporous Materials, 2004. **68**(1–3): p. 77-82.
40. Caullet, P., et al., *The fluoride route: a strategy to crystalline porous materials.* Comptes Rendus Chimie, 2005. **8**(3–4): p. 245-266.
41. Rivera, A., G. Rodríguez-Fuentes, and E. Altshuler, *Characterization and neutralizing properties of a natural zeolite/Na2CO3 composite material.* Microporous and Mesoporous Materials, 1998. **24**(1–3): p. 51-58.
42. J.A. Martens, M.T., P.A. Jacobs and J. Weitkamp, zeolites, 1984. **4**: p. 98.
43. J. Weitkamp, S.E.a.R.K., Appl. Catal, 1986. **27**: p. 207.
44. B.H. Chiche, R.D., F. Di Renzo, F. Fajula, A. Katovic, A. Regina and G. Giordano, Catal. Lett, 1995. **31**: p. 359.
45. L.T.Nemeth, G.F.M., US Pat. 6 872 866, 2005.
46. G. Pazzucconi, C.P., R.Millini, F. Frigerio, R.Mansani, D. Rancati, *Process for the preparation of 2,6-dimethylnaphthalene using a MTW zeolitic catalyst.* US Pat. 6147270, 2000.
47. E.J. Rosinski, M.K.R., US Patent 3970544 1976.
48. Yoo, K., E. Burckle, and P. Smirniotis, *Comparison of protonated zeolites with various dimensionalities for the liquid phase alkylation of i-butane with 2-butene.* Catalysis Letters, 2001. **74**(1-2): p. 85-90.
49. Álvarez-Ayuso, E., A. García-Sánchez, and X. Querol, *Purification of metal electroplating waste waters using zeolites.* Water Research, 2003. **37**(20): p. 4855-4862.
50. Simplício, M., et al., *Permeation of single gases and binary mixtures of hydrogen and helium through a MFI zeolite hollow fibres membrane for application in nuclear fusion.* Separation and Purification Technology, 2014. **122**(0): p. 199-205.
51. Cosoli, P., et al., *Hydrogen sulfide removal from biogas by zeolite adsorption. Part II. MD simulations.* Chemical Engineering Journal, 2008. **145**(1): p. 93-99.
52. Upadek, H. and P. Krings, *Development and Performance of Zeolite-A-Built Non-Phosphate Detergents*, in *Studies in Surface Science and Catalysis*, H.G. Karge and J. Weitkamp, Editors. 1989, Elsevier. p. 701-709.
53. Hertzenberg, E.P. and A.L. Dent, *Zeolites NaHA and CaHA as Toothpaste Abrasives*, in *Studies in Surface Science and Catalysis*, S.H. B. Držaj and S. Pejovnik, Editors. 1985, Elsevier. p. 589-596.
54. Burriesci, N., et al., *Studies on zeolites in agriculture. Effect on crop growth of Prunus persica and Vifis vinifera.* Zeolites, 1984. **4**(4): p. 373-376.
55. Feng, N.-Q. and G.-F. Peng, *Applications of natural zeolite to construction and building materials in China.* Construction and Building Materials, 2005. **19**(8): p. 579-584.
56. Aslam, W., et al., *Selective synthesis of linear alkylbenzene by alkylation of benzene with 1-dodecene over desilicated zeolites.* Catalysis Today, 2014. **227**(0): p. 187-197.
57. Wu, Y., et al., *Enhanced catalytic isomerization of α-pinene over mesoporous zeolite beta of low Si/Al ratio by NaOH treatment.* Microporous and Mesoporous Materials, 2012. **162**(0): p. 168-174.

58. Rahimi, N. and R. Karimzadeh, *Catalytic cracking of hydrocarbons over modified ZSM-5 zeolites to produce light olefins: A review.* Applied Catalysis A: General, 2011. **398**(1–2): p. 1-17.
59. Khowatimy, F.A., et al., *Study of Waste Lubricant Hydrocracking into Fuel Fraction over the Combination of Y-Zeolite and ZnO Catalyst.* Procedia Environmental Sciences, 2014. **20**(0): p. 225-234.
60. Kulprathipanja, S., *Zeolites in Industrial Separation and Catalysis*. 2010: Wiley.
61. Wielers, A.F.H., M. Vaarkamp, and M.F.M. Post, *Relation between properties and performance of zeolites in paraffin cracking.* Journal of Catalysis, 1991. **127**(1): p. 51-66.
62. First, E.L., et al., *Computational characterization of zeolite porous networks: an automated approach.* Physical Chemistry Chemical Physics, 2011. **13**(38): p. 17339-17358.
63. *The Zeolite Framework Database.*[*http://www.iza-structure.org/databases/*](http://www.iza-structure.org/databases/).
64. Thanh, V.G., *Synthesis and Characterization of Nanozeolites*. 2006: Université Laval.
65. Gharibeh, M. and U.o.M.A.C. Engineering, *Microwave Reactor Engineering of Zeolites Synthesis*. 2009: University of Massachusetts Amherst.
66. Ernst, S., et al., *Synthesis of zeolite ZSM-12 in the system (MTEA)2O-Na2O-SiO2-Al2O3-H2O.* Zeolites, 1987. **7**(5): p. 458-462.
67. Barrer, R.M., *Zeolites and their synthesis.* Zeolites, 1981. **1**(3): p. 130-140.
68. Rao, K.J., et al., *Synthesis of Inorganic Solids Using Microwaves.* Chemistry of Materials, 1999. **11**(4): p. 882-895.
69. Brar, T., P. France, and P.G. Smirniotis, *Control of Crystal Size and Distribution of Zeolite A.* Industrial & Engineering Chemistry Research, 2001. **40**(4): p. 1133-1139.
70. S. Cundy, C. and J. Ping Zhao, *Remarkable synergy between microwave heating and the addition of seed crystals in zeolite synthesis-a suggestion verified.* Chemical Communications, 1998(14): p. 1465-1466.
71. Slangen, P.M., J.C. Jansen, and H. van Bekkum, *The effect of ageing on the microwave synthesis of zeolite NaA.* Microporous Materials, 1997. **9**(5–6): p. 259-265.
72. Qin-Hua, C.J.S.D.-K.D.S.-C.H.M.X., *Calcination of Kaolinite and Synthesis of 4A Zeolite Used in Detergent with Microwave Method.* Chin. J. Inorg. Chem, 2000. **16**(5): p. 769.
73. Arafat, A., et al., *Microwave preparation of zeolite Y and ZSM-5.* Zeolites, 1993. **13**(3): p. 162-165.
74. Kang, K.-K., C.-H. Park, and W.-S. Ahn, *Microwave preparation of a titanium-substituted mesoporous molecular sieve.* Catalysis Letters, 1999. **59**(1): p. 45-49.
75. Kooyman, P.J., et al., *Microwave heating in the TS-1 catalyzed oxyfunctionalisation of n-hexane.* Journal of Molecular Catalysis A: Chemical, 1996. **111**(1–2): p. 167-174.
76. Magee, J.S., *Fluid Catalytic Cracking: Science and Technology: Science and Technology*. 1993: Elsevier Science.
77. Zhang, X., et al., *Synthesis of NaX zeolite: Influence of crystallization time, temperature and batch molar ratio SiO2/Al2O3 on the particulate properties of zeolite crystals.* Powder Technology, 2013. **235**(0): p. 322-328.

78. Antonio S. Araujo, A.O.S.S., Marcelo J. B. Souza, Ana C. S. L. S. Coutinho, Joana M. F. B. Aquino, José A. Moura, Anne M. G. Pedrosa, *Crystallization of ZSM-12 Zeolite with Different Si/Al Ratio.* 2005. **11**: p. 159-165.
79. Konno, H., et al., *Effectiveness of nano-scale ZSM-5 zeolite and its deactivation mechanism on catalytic cracking of representative hydrocarbons of naphtha.* Microporous and Mesoporous Materials, 2013. **175**(0): p. 25-33.
80. Hincapie, B.O., et al., *Synthesis of mordenite nanocrystals.* Microporous and Mesoporous Materials, 2004. **67**(1): p. 19-26.
81. Sathupunya, M., E. Gulari, and S. Wongkasemjit, *Microwave preparation of Li-zeolite directly from alumatrane and silatrane.* Materials Chemistry and Physics, 2004. **83**(1): p. 89-95.
82. Zaiku, X., et al., *Influence of alkalinity on particle size distribution and crystalline structure in synthesis of zeolite beta.* Crystal Engineering, 2001. **4**(4): p. 359-372.
83. Mohamed, M.M., et al., *Synthesis of high silica mordenite nanocrystals using o-phenylenediamine template.* Microporous and Mesoporous Materials, 2005. **84**(1–3): p. 84-96.
84. Van Steen, E., L.H. Callanan, and C. Claeys, *Recent Advances in the Science and Technology of Zeolites and Related Materials: Proceedings of the 14th International Zeolite Conference, Cape Town, South Africa, 25-30th April 2004*. 2004: Elsevier.
85. Newman, A.M., *Focus on Solid State Chemistry*. 2007: Nova Science Publishers.
86. Cejka, J., et al., *Introduction to Zeolite Molecular Sieves*. 2007: Elsevier Science.
87. Kamimura, Y., et al., *Synthesis of hydrophobic siliceous ferrierite by using pyridine and sodium fluoride.* Microporous and Mesoporous Materials, 2013. **181**(0): p. 154-159.
88. Du, X., et al., *Cation location and migration in lanthanum-exchanged NaY zeolite.* Chinese Journal of Catalysis, 2013. **34**(8): p. 1599-1607.
89. Jiang, S., et al., *Density functional theory study of relevant properties of lanthanum species and 1-butene activation over lanthanum modified zeolite.* Journal of Molecular Structure: THEOCHEM, 2010. **962**(1–3): p. 1-6.
90. Lee, E.F.T. and L.V.C. Rees, *Calcination of cerium(III) exchanged Y zeolite.* Zeolites, 1987. **7**(5): p. 446-450.
91. Seijger, G.B.F., et al., *Screening of silver and cerium exchanged zeolite catalysts for the lean burn reduction of NOx with propene.* Applied Catalysis B: Environmental, 2003. **40**(1): p. 31-42.
92. Saceda, J.-J.F., et al., *Properties of zeolite Y in various forms and utilization as catalysts or supports for cerium oxide in ethanol oxidation.* Journal of Industrial and Engineering Chemistry, 2012. **18**(1): p. 420-424.
93. Mihályi, R.M., et al., *n-Heptane hydroconversion over nickel-loaded aluminum- and/or boron-containing BEA zeolites prepared by recrystallization of magadiite varieties.* Journal of Molecular Catalysis A: Chemical, 2013. **367**(0): p. 77-88.
94. Howden, M.G., *Zeolite ZSM-5 containing boron instead of aluminium atoms in the framework.* Zeolites, 1985. **5**(5): p. 334-338.
95. Coudurier, G., et al., *Properties of boron-substituted ZSM-5 and ZSM-11 zeolites.* Journal of Catalysis, 1987. **108**(1): p. 1-14.
96. Babitz, S.M., et al., *Monomolecular cracking of n-hexane on Y, MOR, and ZSM-5 zeolites.* Applied Catalysis A: General, 1999. **179**(1–2): p. 71-86.

97. Konno, H., et al., *Kinetics of n-hexane cracking over ZSM-5 zeolites – Effect of crystal size on effectiveness factor and catalyst lifetime.* Chemical Engineering Journal, 2012. **207–208**(0): p. 490-496.
98. Yamaguchi, A., et al., *Deactivation of ZSM-5 zeolite during catalytic steam cracking of n-hexane.* Fuel Processing Technology, 2014. **126**(0): p. 343-349.
99. Xue, N., et al., *1-Butene cracking to propene over P/HZSM-5: Effect of lanthanum.* Journal of Molecular Catalysis A: Chemical, 2010. **327**(1–2): p. 12-19.
100. Lee, J., et al., *Catalytic cracking of C5 raffinate to light olefins over lanthanum-containing phosphorous-modified porous ZSM-5: Effect of lanthanum content.* Fuel Processing Technology, 2013. **109**(0): p. 189-195.
101. Karge, H.G., et al., *Cracking of n-decane over Lanthanum Y catalysts: Comparison of Lanthanum Y catalysts obtained by solid-state ion exchange and ion exchange in solution.* Applied Catalysis, 1991. **75**(1): p. 343-357.
102. Varzaneh, A.Z., J. Towfighi, and A. Mohamadalizadeh, *Comparative study of naphtha cracking over SAPO-34 and HZSM-5: Effects of cerium and zirconium on the catalytic performance.* Journal of Analytical and Applied Pyrolysis, 2014. **107**(0): p. 165-173.
103. Suryanarayana, C. and G. Norton, *X-Ray Diffraction: A Practical Approach*. 1998: Springer.
104. Koch, C., et al., *Structural Nanocrystalline Materials: Fundamentals and Applications*. 2007: Cambridge University Press.
105. Do, D.D., *Adsorption Analysis: Equilibria and Kinetics*. 1998: World Scientific Publishing Company Incorporated.
106. Corma, A., *From Microporous to Mesoporous Molecular Sieve Materials and Their Use in Catalysis.* Chemical Reviews, 1997. **97**(6): p. 2373-2420.
107. Gopal, S., K. Yoo, and P.G. Smirniotis, *Synthesis of Al-rich ZSM-12 using TEAOH as template.* Microporous and Mesoporous Materials, 2001. **49**(1–3): p. 149-156.
108. Kamimura, Y., K. Itabashi, and T. Okubo, *Seed-assisted, OSDA-free synthesis of MTW-type zeolite and "Green MTW" from sodium aluminosilicate gel systems.* Microporous and Mesoporous Materials, 2012. **147**(1): p. 149-156.
109. Frank Lai, R.B.S., Kathy Saunders, US 2011/0118520 A1, May 19, 2011.
110. Rodríguez-González, L., et al., *The acid properties of H-ZSM-5 as studied by NH3-TPD and 27Al-MAS-NMR spectroscopy.* Applied Catalysis A: General, 2007. **328**(2): p. 174-182.
111. Zhang, C., et al., *Effects of steam and TEOS modification on HZSM-5 zeolite for 2,6-dimethylnaphthalene synthesis by methylation of 2-methylnaphthalene with methanol.* Catalysis Today, 2010. **149**(1–2): p. 196-201.
112. Rao, G.N. and A.N. Kotasthane, *Thermal and hydrothermal stabilities of zeolite EU-1.* Applied Catalysis A: General, 1994. **119**(1): p. 33-43.
113. Lutz, W., et al., *Investigation and Modeling of the Hydrothermal Stability of Technically Relevant Zeolites.* Adsorption, 2005. **11**(3-4): p. 405-413.
114. Ravenelle, R.M., et al., *Stability of Zeolites in Hot Liquid Water.* The Journal of Physical Chemistry C, 2010. **114**(46): p. 19582-19595.
115. Lutz, W., et al., *Hydrothermal stability of zeolite SAPO-11.* Microporous and Mesoporous Materials, 2010. **132**(1–2): p. 31-36.

116. Triantafillidis, C.S., A.G. Vlessidis, and N.P. Evmiridis, *Dealuminated H−Y Zeolites: Influence of the Degree and the Type of Dealumination Method on the Structural and Acidic Characteristics of H−Y Zeolites.* Industrial & Engineering Chemistry Research, 1999. **39**(2): p. 307-319.

Vitae

Name : Mohammed Ahmed Sanhoob

Nationality : Yemeni

Date of Birth : September 26, 1987

Email : m.sunhope@gmail.com

Address : Dhahran- King Fahd University of Petroleum and Minerals

Academic Background : Chemical engineer

Publications:

1. Mohammed Sanhoob, O. Muraza, E.M. Al-Mutairi, B. Merzougui, Z. H. Yamani, T. Tago, T. Masuda, Synthesis of ZSM-12 with different Al-sources: Towards understanding the crystallization parameters, Microporous and Mesoporous Materials 194 (2014) 31-37. Impact factor = 3.209.

2. Mohammed A. Sanhoob, Oki Muraza, Eid M. Al-Mutairi, Nisar Ullah, Role of crystal growth modifiers in the synthesis of ZSM-12 zeolite, Advanced Powder Technology, Accepted. Impact factor = 1.642.

3. Jamil, A.K., et al., Controlling naphtha cracking using nanosized TON zeolite synthesized in the presence of polyoxyethylene surfactant. Journal of Analytical and Applied Pyrolysis, 2014. 110(0): p. 338-345.Impact factor =3.070.

4. O. Muraza, Mohammed Sanhoob, M. Abdul Bari Siddiqui, Development of desilicated MTW zeolite and its application in catalytic cracking of n-heptane, Journal of Analytical and Applied Pyrolysis, Submitted.

5. Mohammed Sanhoob, O. Muraza, M. Abdul Bari Siddiqui, Catalytic cracking of La, Ce and B-MTW, Under preparation.

Conferences:

1. M. Sanhoob, O. Muraza, E.M. Al-Mutairi, B. Merzougui, Z. H. Yamani, T. Tago, T. Masuda, Synthesis of ZSM-12 with different Al-sources: Towards understanding the crystallization parameters, Book of Abstract of *Pre-Symposium* of ZMPC 2012, *Kyoto,* 26-27 July 2012.

2. O. Muraza, A.K. Jamil, M. Sanhoob, A.M. Al-Amer, T. Tago, H. Konno, Y. Nakasaka, T. Masuda, Nanosized Ton Zeolite Synthesized in the Presence of Polyoxyethylene Surfactant and Its Application in N-Hexane Cracking, Procedding of the Sixth Asia-Pacific Congress on Catalysis (APCAT-6) in Taipei, Taiwan in October 13 - 17, 2013.